OCEAN UPTAKE OF CARBON DIOXIDE †

Tsung-Hung Peng
Environmental Sciences Division
Oak Ridge National Laboratory
P. O. Box 2008
Oak Ridge, Tennessee 37831–6335

and

Taro Takahashi
Lamont-Doherty Earth Observatory
of Columbia University
Palisades, New York 10964

† Research sponsored by U.S. Department of Energy, Carbon Dioxide Research Program, Environmental Sciences Division, Office of Health and Environmental Research, under contract DE–AC05–84OR21400 with Martin Marietta Energy Systems, Inc.

OCEAN UPTAKE OF CARBON DIOXIDE

Tsung-Hung Peng
Environmental Sciences Division
Oak Ridge National Laboratory
Oak Ridge, Tennessee 37831

and

Taro Takahashi
Lamont-Doherty Earth Observatory of Columbia University
Palisades, New York 10964

Abstract

Factors controlling the capacity of the ocean for taking up anthropogenic CO_2 include carbon chemistry, distribution of alkalinity, pCO_2 and total concentration of dissolved CO_2, sea-air pCO_2 difference, gas exchange rate across the sea-air interface, biological carbon pump, ocean water circulation and mixing, and dissolution of carbonate in deep sea sediments. A general review of these processes is given and models of ocean-atmosphere system based on our understanding of these regulating processes are used to estimate the magnitude of CO_2 uptake by the ocean. We conclude that the ocean can absorb up to 35% of the fossil fuel emission. Direct measurements show that 55% of CO_2 from fossil fuel burning remains in the atmosphere. The remaining 10% is not accounted for by atmospheric increases and ocean uptake. In addition, it is estimated that an amount equivalent to 30% of recent annual fossil fuel emissions is released into the atmosphere as a result of deforestation and farming. To balance global carbon budget, a sizable carbon sink besides the ocean is needed. Storage of carbon in terrestrial biosphere as a result of CO_2 fertilization is a potential candidate for such missing carbon sinks.

Introduction

One recent serious environmental concern is the possibility of climate change caused by the steady buildup of carbon dioxide and other greenhouse gases in our atmosphere. Interest in this question has stimulated consideration of the long term fate of gases that are added to the atmosphere as a result of human activities. As carbon dioxide is the chief villain and is the most stable greenhouse gas, its possible fate has received the most attention. Through the burning of oil, natural gas, and coal, currently 5.5 giga tons of carbon (GtC) in the form of CO_2 are released to the atmosphere each year. Where does all this CO_2 go? Atmospheric observations show that the rate at which CO_2 is building up in the

atmosphere is just a bit more than half that expected if all the CO_2 released by burning fossil fuels remained airborne. This fraction becomes even smaller when the CO_2 being added to the atmosphere as the result of deforestation is taken into account. Terrestrial ecologists give an estimate of 1 to 2 GtC that are produced each year by cutting and burning trees. With the atmospheric CO_2 increasing at the current rate of 3.4 GtC per year, we have about 3.6 GtC to account for.

Oceans are the first suspects that can take up a large amount of missing carbon. The ocean is a large dynamic CO_2 reservoir containing about 50 times as much CO_2 as the atmosphere. Hence, it plays a major role in regulating the concentration of atmospheric CO_2 over a wide range of time scales, from a year or less to many centuries. A broad picture of our current understanding of the processes governing the capacity of the oceanic carbon reservoir for taking up anthropogenic CO_2 is reviewed in the following sections. The attempt to account for the global CO_2 budget involving terrestrial biosphere is also given at the last section. The general conclusion is that the ocean can account for 2 GtC per year and the terrestrial carbon sinks can potentially take up an extra of about 1.5 GtC per year.

Carbon Chemistry in The Ocean

The chemical reactions between CO_2 gas and seawater may be expressed by the following:

$$CO_2(\text{gas}) + H_2O \rightarrow H_2CO_3(\text{aq}), \tag{1}$$

$$H_2CO_3 \rightarrow H^+ + HCO_3^-, \text{and} \tag{2}$$

$$HCO_3^- \rightarrow H^+ + CO_3^{2-}. \tag{3}$$

The equilibrium constants for these reversible reactions are defined by

$$K_0' = [H_2CO_3]/pCO_2 \tag{4}$$

$$K_1' = aH^+[HCO_3^-]/[H_2CO_3] \tag{5}$$

$$K_2' = aH^+[CO_3^{2-}]/[HCO_3^-] \tag{6}$$

where K_0' is the solubility of CO_2 in seawater, K_1' and K_2' are the first and second apparent dissociation constants of carbonic acid in seawater, pCO_2 is the partial pressure of CO_2 exerted by seawater, and aH^+ is the activity of the hydrogen ion in seawater. Furthermore, the brackets indicate the concentrations. The values of solubility and apparent dissociation constants in seawater differ substantially from those determined for pure water, as shown

in the Table 1. In this table, K indicates the values for pure water, and K' indicates a typical seawater with a salinity of 35.00°/$_{oo}$ under a total pressure of 1 atm. The first and second dissociation constants in pure water are those determined respectively by Harned and Davis (1943) and by Harned and Scholes (1941); the solubility values are based on the measurements of Murray and Riley (1971). The empirical equations, formulated by Weiss (1974) for the solubility of CO_2 and by Millero (1979) for the dissociation constants, may be conveniently used to compute these values as a function of temperature and salinity.

The solubility of CO_2 decreases with increasing salinity, much like the solubility of other atmospheric gases (such as oxygen, nitrogen, and argon) mainly because of the effects of ionized salt species in seawater. On the other hand, both the first and second dissociation constants increase appreciably as salinity increases. This increase in the constants has been attributed mainly to ion associations (or the formation of complex ions) such as $Mg(HCO_3)^+$, $Na(HCO_3)^0$, and $Ca(CO_3)^0$ (e.g., Garrels and Thompson, 1962; Garrels and Christ, 1965; Simpson and Takahashi, 1973).

When the solubility of CO_2 and the apparent dissociation constants in seawater are known at a given temperature and salinity, at least two of the following four measurable quantities must also be known in order to determine the system: the total concentration of CO_2 species dissolved in seawater, alkalinity, pCO_2, and pH. A computational scheme and various empirical equations representing equilibrium constants as a function of temperature and salinity are summarized in Peng et al. (1987).

The total CO_2 concentration (TCO_2) is the sum of all the CO_2 species dissolved in seawater:

$$TCO_2 = K_0' \, pCO_2 + [HCO_3^-] + [CO_3^{2-}] \tag{7}$$

where the quantities in [ ] indicate the concentrations of the indicated species, including the free and complexed ions. The total CO_2 concentration corresponds to the amount of CO_2 gas extractable from an acidified seawater sample. This quantity may be determined by means of manometric, gas chromatographic, coulometric, titrimetric methods with a precision as good as ±0.05%. In the oceans, the total CO_2 concentration may be mainly altered by sea-air gas exchange, biological utilization/respiration, $CaCO_3$ precipitation/dissolution, and mixing between the different water masses.

The alkalinity is a measure of ionic charges carried by the dissociation in seawater of weak acids such as carbonic, boric, silicic and phosphoric acids. It is based on the statement of

charge balance:

$$\{[Na^+] + [K^+] + 2[Mg^{2+}] + 2[Ca^{2+}] + \cdots\} + [H^+]$$
$$= \{[Cl^-] + 2[SO_4^{2-}] + [NO_3^-] + \cdots\} + [HCO_3^-] + 2[CO_3^{2-}]$$
$$+ [H_2BO_3^-] + [H_3SiO_4^-] + \cdots + [OH^-]$$

where the braces { } are used to group the species whose concentrations are independent of hydrogen ion concentration. In seawater, the sum of cationic charges in the braces exceeds that of anionic charges in the braces, and the excess cationic charge is balanced by the anionic charge generated by dissociation of the weak acids and water. The amount of this excess charge, called alkalinity, is expressed by

$$ALK = \{[Na^+] + [K^+] + 2[Mg^{2+}] + 2[Ca^{2+}] + \cdots\} - \{[Cl^-] + 2[SO_4^{2-}] + [NO_3^-] + \cdots\} \quad (8a)$$
$$= [HCO_3^-] + 2[CO_3^{2-}] + [H_2BO_3^-] + [H_3SiO_4^-] + \cdots + [OH^-] - [H^+] \quad (8b)$$

The alkalinity is therefore equal to the equivalence of acid that is required to drive all the weak acids in Eq. (8b) to undissociated forms such as H_2CO_3 and H_3BO_3. Eq. (8a) shows that the alkalinity depends only on the concentrations of the strong electrolyte species and hence is independent of temperature and pressure. However, the pH and proportions of dissociated weak acids are altered by changes in temperature and pressure. The alkalinity in seawater may be determined with a high degree of precision (± 2 μeq/kg) by means of the potentiometric acid titration method (e.g., Gran, 1952 and Bradshaw et al.,1981).

The alkalinity may be altered by a number of processes in the oceans. When NO_3^- is consumed by photosynthesis, the alkalinity is increased by a corresponding amount (Brewer and Goldman, 1976), as seen in Eq. (8a). The precipitation of $CaCO_3$ by shell-secreting marine organisms such as foraminifera and coccoliths decreases the alkalinity: the removal of 1 mol of $CaCO_3$ from seawater decreases the alkalinity by 2 equivalents and decreases the total CO_2 concentration by 1 mol. On the other hand, the posthumous dissolution of the skeletal $CaCO_3$ in deep oceans increases the alkalinity as well as the CO_2 concentration in deep waters. The alkalinity remains unaffected by the precipitation or dissolution of gypsum ($CaSO_4 \cdot 2H_2O$) or anhydride ($CaSO_4$) from seawater, because changes in Ca^{2+} and SO_4^{2-} with a 1:1 stoichiometric ratio cancel each other, as seen in Eq. (8a). An addition of CO_2 would not affect the alkalinity in seawater, according to Eq. (8a), but would result in changes of the pH and proportions of the dissociated species.

The gravitational settling of biogenic $CaCO_3$ and its dissolution in deep waters constitute a major biogeochemical pathway in the oceanic carbon cycle. For this reason, alkalinity

is not only a necessary quantity for determining the carbonate chemistry in seawater but also an important tracer for the investigation of the $CaCO_3$ cycle in the oceans.

The partial pressure of CO_2 (pCO_2) is a measure of the dissolved CO_2 species in seawater [see Eqs. (1) and (4)], representing the thermodynamic driving potential for sea-air gas exchange. Thus, it is important in the investigation of gas transfer between the atmosphere and oceans. It may be measured by analyzing the CO_2 concentration or partial pressure in the air sample equilibrated with a sample of seawater at a known temperature and pressure. The gas chromatograph (Weiss, 1981) and nondispersive infrared gas analyzer (Broecker and Takahashi, 1966) have often been used for the measurement of pCO_2 with a precision of $\pm 0.3\%$ (Takahashi et al., 1982).

For surface waters of the global ocean, where the temperature (T) ranges from about -1 to 30°C and salinity (S) from about 32 to 36°/$_{oo}$, the effect of temperature on pCO_2 is nearly constant in this temperature and salinity range:

$$(\partial \ln pCO_2/\partial T)_{ALK,TCO_2,S} = 0.043\ ^oC^{-1} \tag{9}$$

where $(\partial \ln pCO_2)$ is used to express $(\partial pCO_2/pCO_2)$ more conveniently. This means that pCO_2 in seawater doubles with a temperature increase of every 16°C.

In addition, the pCO_2 in seawater is sensitively affected by the alkalinity and total CO_2 concentration, both of which may be changed through biological processes. The following equations express the effects of total CO_2 concentration, alkalinity, and salinity respectively:

$$(\partial \ln pCO_2/\partial \ln TCO_2)_{ALK,S,T} = 10 \tag{10}$$

for global surface water average (8 for warm and 14 for cold waters, Takahashi et al., 1980)

$$(\partial \ln pCO_2/\partial \ln ALK)_{TCO_2,S,T} = -9.4 \tag{11}$$

for global surface water average (-7.4 for warm and -13.3 for cold waters)

$$(\partial \ln pCO_2/\partial \ln S)_{ALK,TCO_2,T} = 0.94 \tag{12}$$

for global surface water average (0.93 for warm and 1.0 for cold waters)

The quantity expressed by Eq. (10) is often referred to as the Revelle factor (Revelle and Suess, 1957). It means that a 1% increase in the total CO_2 concentration in the global mean surface seawater causes the pCO_2 to increase by 10%. On the other hand, a 1% increase in the alkalinity causes the pCO_2 to decrease by 9.4%.

The pH of seawater is well buffered at about 8.1 mainly because of the presence of carbonic and boric acids. Nevertheless, highly precise and reproducible measurements of pH in natural seawater are difficult to make, particularly under shipboard conditions. A hydrogen electrode cannot be used because the hydrogen gas used to flush the platinum electrode sweeps CO_2 out of the seawater sample and thus changes the CO_2 concentration and the pH. A glass-calomel reference electrode pair also has problems: its response may be affected by a liquid-junction potential as well as by a trace of various organic compounds present in seawater, which may be adsorbed onto the surface of the electrode. Furthermore, it is not certain whether the glass electrode responds exclusively to the H^+ ion activity or the H^+ ion concentration, or to a quantity related to both of these (Bates and Culberson, 1977).

Whatever the physical meaning of the electrode response, the most important requirement for the pH measurement in oceanic CO_2 studies is that the measurements be consistent with those performed for the determination of the first and second dissociation constants of carbonic acid in seawater. Furthermore, it is necessary to measure pH as precise as 0.001 pH unit in order to obtain a computed pCO_2 value with a precision of 1 μatm, which is comparable to that for shipboard pCO_2 measurements. This level of precision in pH measurements during oceanographic expeditions has not yet been sustained for periods as long as several years.

In contrast to the alkalinity and total CO_2 concentration, the pH of a parcel of seawater depends on temperature and pressure, as well as on alkalinity and total CO_2 concentration. Therefore, the usefulness of pH as an oceanographic tracer is limited.

Distribution of CO_2 In The Oceans

Because of mounting concern about climatic warming induced by atmosph
tion of industrial CO_2 and because of the oceans' role as a large dynami
the distribution of CO_2 and its related quantities in the global oceans has b
extensively in recent years, particularly since the early 1970s. The results of
(Geochemical Ocean Sections Study) Program conducted in 1972-1978 are show
1 to illustrate the depth distribution of the total CO_2 concentration (TCO_2) and
linity (ALK) in various regions of the global oceans (Takahashi et al., 1981a; see Takahashi et al. (1981b) for the listing of the mean regional values). These data were obtained by using the potentiometric acid titration method described by Bradshaw et al. (1981).

The mean values for alkalinity and total CO_2 concentration in surface waters (Table 2) yield a pCO_2 value of 309 μatm at the mean surface water temperature of 19.2°C. This value indicates that the mean surface water was undersaturated by about 4% in relation to the atmosphere, which had a pCO_2 of 321 ($\pm$3) μatm in 1973, when these oceanic measurements were made. On the other hand, the mean alkalinity and total CO_2 concentration for the whole ocean yield a pCO_2 value of 437 μatm at the mean deep water temperature of 1.5°C and a value of 913 μatm at the mean surface water temperature of 19.2°C. This indicates that the deep ocean water is highly supersaturated with respect to atmospheric CO_2. If the atmosphere were brought to equilibrium with a hypothetical ocean chemically homogenized at the mean whole ocean temperature of 3.9°C (Table 2) the atmospheric pCO_2 value would increase by about 40%. If the temperature were to increase to the mean surface water temperature of 19.2°C, the atmospheric pCO_2 would increase almost three fold. The unique feature of the oceans is that a large body of deep water that is highly supersaturated with respect to atmospheric CO_2 is capped with a relatively thin layer of warmer and less dense seawater that retards the exchange of CO_2 between these reservoirs. Understanding of this "sequestering" process for CO_2 in deep ocean water is one of the central questions in the investigation of oceanic CO_2.

Figure 1 shows that the total CO_2 concentration in seawater increases rapidly with increasing depth from the surface to about 1000 m; below 1000m, it changes more slowly. This variation may be accounted for by the existence of a biological carbon pump, which transports CO_2 from the upper layers to the deep ocean through the gravitational settling of biogenic debris produced by photosynthesis in the photic zone of the oceans. The debris is mostly oxidized during its sinking through the water column. The fact that the organic carbon content in deep ocean sediments is low (i.e., less than 1 weight percent) indicates that only a small portion of the biogenic debris reaches the sea floor. Figure 1 also shows that the alkalinity increases with depth less rapidly than the total CO_2 concentration. In the profiles for Pacific and Indian oceans, the alkalinity gradient is reduced significantly at the depths around 2000 m, whereas a similar change in the total CO_2 gradient occurs at the depths around 1000 m. These changes in the gradients suggest that, while organic debris (such as soft tissues) oxidize at all the depths in the water column (presumably more rapidly in the warmer upper waters), the hard calcareous shells dissolve only in deep oceans below certain water depths. It has been observed that the deep sea floor of the Atlantic Ocean with water depths shallower than about 4500 m is covered with a layer of calcareous mud (or "ooze") consisting mainly of foraminifera shells; in contrast, the deep sea sediments of the Atlantic deeper than 4500 m and those of virtually the entire

North Pacific Ocean (except the shallow areas surrounding seamounts) are nearly devoid of $CaCO_3$. This difference occurs mainly because the solubility of $CaCO_3$ (i.e., the minerals calcite or aragonite) increases rapidly with pressure (Ingle et al., 1973; Ingle, 1975) as shown in Figure 2: the solubility product doubles with a pressure increase of about 430 atm (or about 4300 m in water depth). The seawater in the surface layer is generally supersaturated several fold with respect to calcite. It becomes undersaturated with respect to calcite (i.e., the shells of coccoliths and foraminifera) below a depth of about 4500 m in the Atlantic Ocean and a depth between 1000 and 3000 m in the Pacific Ocean due mainly to a combination of two effects: an increase in the solubility under greater pressures and a nearly constant CO_3^{2-} ion concentration in seawater at depths below about 2000 m (Figure 2). The regional difference in undersaturation depths is attributed to the difference in the total CO_2 concentration and alkalinity in deep waters (Takahashi, 1975; Broecker and Takahashi, 1978).

Gas Transfer Between The Atmosphere And The Oceans

Because the exchange of CO_2 between the atmosphere and the oceans occurs across the sea-air interface, the magnitude and the distribution of the transfer flux over the global oceans are key components in the CO_2 cycle. Since direct measurements of the net CO_2 flux (F) across the sea surface are not yet possible, the flux is generally computed by

$$F = E \cdot \Delta pCO_2 \tag{13}$$

where ΔpCO_2 is the difference between the CO_2 partial pressure in seawater and that in the overlying air, and it represents the thermodynamic potential for gas transfer. E is the gas transfer coefficient across the sea-air interface and depends mainly on wind speed.

The gas transfer coefficient (E) in Eq. (13) depends on the degree of turbulence in the surface layer of the ocean and the overlying air and may be expressed as a function of the gas exchange piston velocity (Vp), which is affected by the wind speed, and the solubility of CO_2 in seawater (Sb), which depends mainly upon water temperature:

$$E = Vp \cdot Sb \tag{14}$$

Vp, in turn, is not only related to wind speed, but also proportional to the molecular diffusivity (D) of CO_2 in seawater and the viscosity of water (ν) :

$$Vp \propto (D/\nu)^{1/2}, \text{ where the wind speed is constant.} \tag{15}$$

In a typical oceanic temperature range of 0 to 25°C, D increases by a factor of 2 with temperature increase, while ν decreases by a factor of 2. Therefore, Vp increases by a

factor of 2. However, Sb also decreases by a factor of 2. Hence, the effects of temperature on Vp and Sb cancel each other and E becomes mainly a function of wind speed alone.

A number of investigators have studied the wind dependence of E under field conditions as well as in the laboratory with various wind tunnel devices (see reviews by Broecker et al, 1986b; Liss and Merlivat, 1986). It has been observed that the transfer coefficient Vp increases very slowly up to a wind speed of about 3 m s^{-1} (Fig. 3). At higher wind speeds it increases linearly with increasing wind speed. However, the dependence of Vp on wind speed observed using various wind tunnels and in the field varies over a wide range as shown in Fig. 3: the dashed and solid lines indicate the limits of the wind tunnel data, and the circles and squares indicate the field data obtained using the distribution of radon gas and ^{14}C, respectively. The results obtained for a lake environment by using the SF_6 spike method (Wanninkhof et al., 1985) are consistent with the lower limit of the wind tunnel results, represented by the solid lines. The solid lines also represent the wind speed dependence calculated by Liss and Merlivat (1986) on the basis of this agreement. Although the wide range of the wind tunnel data must be related to the shape of waves generated and to the ways in which the turbulent air and water interact, the cause of the differences has not been clearly understood.

The global mean CO_2 exchange rate in the open ocean has been estimated on the basis of the distribution of natural ^{14}C in the air and the sea. Radiocarbon is produced in the upper atmosphere and is taken up as $^{14}CO_2$ by the oceans, where it decays. Because the $^{14}C/^{12}C$ ratio in the atmosphere has been nearly constant over the last 2000 years, as documented by ^{14}C measurements on tree rings (Klein et al., 1982), the ^{14}C distribution in the atmosphere-ocean system appears to be in steady state: the radioactive decay rate of ^{14}C (5730 year half-life) within the sea is matched by the net transport rate of ^{14}C into the sea across the sea-air interface. On the basis of the best estimates of the ^{14}C data for a period prior to the industrial revolution (Broecker and Li, 1970; Oeschger et al., 1975), the CO_2 exchange rate has been estimated to be 19±5 mol $m^{-2}yr^{-1}$. Taking the preindustrial atmospheric pCO_2 value to be 274 μatm (with a 2% correction for the water vapor pressure applied to 280 ppm mole fraction in dry air), the corresponding values for E and Vp are 0.069±0.018 mol $m^{-2}yr^{-1}\mu atm^{-1}$ and 5.7±1.5 m day^{-1}, respectively, at a global mean sea surface temperature of 19°C. This Vp value is shown with a square symbol in Fig. 3.

The global mean CO_2 exchange rate may also be estimated by using a transient increase of ^{14}C in the atmosphere and the oceans as result of the atmospheric nuclear bomb tests in the 1960s. The measurements by Nydal and Lovseth (1983) indicate that the atmospheric

^{14}C level reached a maximum value of 100% over the prebomb value during the period 1963-1964. Since then, it has declined slowly because of its transfer into the oceans, and the ^{14}C activity in the surface ocean water has increased steadily. Using this information, Stuiver (1980) has estimated the mean CO_2 exchange rate for the Atlantic Ocean from 40°N to 40°S to be 23±3 mol $m^{-2}yr^{-1}$. Under the assumption that the mean atmospheric pCO_2 value was 320 μatm during the 10-year period between 1963 and 1973, this exchange rate corresponds to an E value of 0.072±0.01 mol $m^{-2}yr^{-1}\mu atm^{-1}$ or a Vp value of 6.0±0.8 m day^{-1}. This Vp value is also shown with a square in Fig. 3.

Whereas the ^{14}C methods discussed above yield estimates for gas transfer rates averaged over the global or regional scale for a period of a decade to centuries, measurements of radon deficiencies in surface ocean water yield estimates for a local Vp value averaged over a period of weeks (i.e., several times of the ^{222}Rn decay half-life of 3.83 days). Produced in the surface water by the radioactive decay of ^{226}Ra, ^{222}Rn escapes to the atmosphere, where its concentration is generally very low. Thus, the concentration of ^{222}Rn in near surface waters is less than that in equilibrium with ^{226}Ra. Because the magnitude of radon deficiency depends on the rate of gas exchange, a Vp value may be computed under the assumption that the distribution of ^{222}Rn in the water column is in steady state (Roether and Kromer, 1984). Based on radon profiles measured over 100 stations in the Atlantic and Pacific oceans during the GEOSECS program, the global mean Vp value of 2.9 m day^{-1} for radon (at 20°C) has been obtained (Peng et al., 1979a). This Vp value corresponds to 3.5 m day^{-1} for CO_2, as is shown with a circle in Fig. 3. The Vp values estimated on the basis of radon deficiencies at various locations are also indicated with circles in the same figure. With the exceptions of the data obtained during the JASIN program (Roether and Kromer, 1984), these values tend to be more consistent with the lower limit of the wind tunnel data.

As reviewed above, the dependence of Vp on wind speed is presently known only to within a factor of 2. However, for the purpose of computing the global CO_2 flux across the sea-air interface by using Eq. (13), the following relationship is assumed:

$$\text{Vp (m day}^{-1}) = 1.4\ [\text{W(m s}^{-1}) - 3],\ \text{for } CO_2 \text{ at } 20°C \qquad (16a)$$

and

$$\text{E(mol } CO_2 \text{ m}^{-2} \text{ yr}^{-1} \mu\text{atm}^{-1}) = 0.016\ [\text{W(m s}^{-1}) - 3], \qquad (16b)$$

where W is the wind speed in m s^{-1}. Equation (16a) is plotted on Fig. 3 with a short dashed line. As noted earlier, E is assumed to be independent of temperature. These

two relationships have been chosen here for two reasons. First, the global mean CO_2 exchange rates determined on the basis of the steady-state distribution of natural ^{14}C and the transient distribution of bomb-produced ^{14}C are free of weak assumptions and hence are robust. Second, the ^{14}C atoms in the atmosphere and oceans exist as $^{14}CO_2$; thus the estimated rate reflects directly that of CO_2.

The ΔpCO_2 has been mapped over the global oceans during the 1972-1978 GEOSECS Program (Fig. 4). The positive values in ΔpCO_2 indicate areas that are sources for atmospheric CO_2, whereas the negative values indicate areas that are sinks for atmospheric CO_2. Because the variability of pCO_2 values in the ocean is far greater than that in the atmosphere, the observed variations in ΔpCO_2 reflect mainly those in the oceanic pCO_2 values. Furthermore, this map represents a summary of the measurements made during the oceanographic expeditions undertaken mostly during the summer months in the high-latitude areas in the northern and southern hemispheres and during other seasons in the middle- to low-latitude areas. Therefore, the map is not intended to show a synoptic distribution. Yet, the following major features are apparent: (1) The global surface ocean water is out of thermodynamic equilibrium with atmospheric CO_2 by as much as 25%. This suggests that the gas transfer rate across the sea-air interface is slow in comparison with changes in pCO_2 in seawater. (2) The equatorial Pacific and Atlantic oceans are strong sources. (3) The area between about 30°S and 55°S in the South Atlantic is strong sink, as indicated by large negative values in ΔpCO_2. (4) The northern high-latitude areas, including the Norwegian and the Greenland seas and the North Atlantic Ocean north of about 40°N, are strong CO_2 sinks during the summer months.

A systematic pCO_2 increase in the surface waters of the temperate gyre in the North Atlantic Ocean (i.e., the Sargasso Sea) has been observed over the past two decades (Takahashi et al., 1983). The mean pCO_2 in the surface water during the three expeditions in the period from 1957 to 1981 (Fig. 5) shows that the pCO_2 values measured during different seasons correlates linearly with temperature. In order to minimize the bias for seasonal difference, the mean pCO_2 has been estimated from the pCO_2 value computed for a mean temperature of 19.6°C by using the pCO_2-temperature regression equations for each of the three expeditions. Fig. 5 shows that the pCO_2 has increased at a mean rate of 1.5 μatm per year between 1957 and 1981; furthermore, this rate is nearly consistent with that in the atmosphere (Bacastow and Keeling, 1981). Thus, it appears that the gyre water has taken up anthropogenic CO_2 from the air.

Global CO_2 Flux Across the Sea Surface

Using Eq. (13), Tans et al. (1990) computed the seasonal and annual CO_2 flux across the sea-air interface for the global oceans on the basis of recent estimates of sea-air ΔpCO_2 over various oceanographic regions (Table 3). The CO_2 transfer coefficient (E) was computed by using Eq. (16b) and the climatological wind speeds compiled by Esbensen and Koshnir (1981) for the global oceans. The mean global sea-air CO_2 exchange coefficient thus estimated is 0.067 mol CO_2 $m^{-2}yr^{-1}\mu atm^{-1}$, which is consistent with the global mean CO_2 exchange rate of 20 ± 3 mol$\cdot m^{-2}\cdot yr^{-1}$ obtained on the basis of the ^{14}C inventory in the atmosphere-ocean system (Broecker et al., 1986b).

The global CO_2 flux summarized in Table 3 indicates that the winter net flux into the ocean is 1.5 GtC yr^{-1}, and the summer net flux is 1.7 GtC yr^{-1}, with a mean annual ocean uptake of 1.6 GtC yr^{-1}. These values would be halved if the constant in Eq. (16b) for E is replaced with the value derived by using Liss and Merlivat (1986) linear relationship between Vp and W. The results of annual flux shown in this Table indicate that equatorial ocean is the single oceanic source, mainly because of the upwelling of deep waters, whereas the southern ocean gyres including Atlantic, Pacific and Indian oceans are major CO_2 sinks, accounting for about 75% of the total global oceanic sink flux. Because the fossil fuel sources are located mainly in the northern hemisphere, the large southern hemisphere oceanic uptake requires a large interhemispheric CO_2 transport within the atmosphere. Based on the observed interhemispheric CO_2 gradient in the atmosphere, such a large interhemispheric transport is not supported (Tans et al. 1990). The estimated net oceanic CO_2 flux of 1.6 GtC per year from the atmosphere to the oceans suggests that about 30% of the annual industrial CO_2 emissions (a mean of 5.4 GtC for the period 1980-89) is taken up by the oceans. The observed airborne fraction, 0.55, of the industrial emissions (Bacastow and Keeling, 1981) suggests that a discrepancy of about 15% is unaccounted for (missing carbon). These problems suggest that the CO_2 uptake rate presented in Table 3 is poorly constrained because of the following reasons.

1. The wind speed dependence of the gas transfer coefficient is not well known (Fig. 3).

2. Only a limited number of the oceanic pCO_2 measurements are available in the high-latitude Southern Ocean during the winter months, in particular the Pacific and Indian Ocean sectors, mainly because of the limited accessibility. Presently, information on these areas is deduced mainly from a small number of measurements and the knowledge acquired in the Atlantic sector of the Southern Ocean.

3. The gas exchange in the sea-ice covered areas of the oceans is poorly understood. In this study, it has been assumed that the sea-air gas exchange is totally impeded by the sea ice cover in the high- latitude oceans south of 60°S and north of 70°N during the winter. However, it is well known that numerous small open areas of ocean water (i.e., polynyas) are present within the ice fields as well as along the coastal areas of the Antarctica. In these areas, CO_2 must be exchanged vigorously between the atmosphere and seawater because of the strong turbulence associated with ice margins. Further studies are needed to improve our knowledge of the gas exchange in the ice-covered areas.

The improvements in estimating the global sea-air CO_2 fluxes will be possible under oceanography programs to be conducted from space. For example, sea surface roughness will be mapped by a radar scatterometer (or possibly an optical device) aboard future satellites. Furthermore, ground-truth experiments are being planned so that the sea surface roughness can be correlated with the wind speed and with the sea-air gas transfer coefficient. Ocean color measurements in a range sensitive to chlorophyll will be used to determine the production rate of marine phytoplankton, which is one of the important factors governing the sea-air pCO_2 difference.

Neutralization Of Anthropogenic CO_2 By Marine Sediments

Surface ocean water will become more acidic as it absorbs anthropogenic CO_2. The down ward mixing of the surface water enriched with this industrial CO_2 will gradually acidify the deep ocean water. However, this excess acid will be neutralized by the dissolution of skeletal $CaCO_3$ in the deep sea sediments which are in contact with the acidified water. Coastal and shallow water deposits are less important for the neutralization reaction because of their smaller area and their lower $CaCO_3$ content, with the exception of coral reef deposits. Furthermore, the upper layers of temperate and tropical oceans, where coral reefs are found, are presently several fold supersaturated with respect to calcite and aragonite (see Figure 2). These waters will not become undersaturated until the total CO_2 concentration in the surface water is increased by about 15% (or from 2000 to 2300 μmol/kg), causing the surface water pCO_2 to increase by as much as 8 fold (or from 330 to 2800 μatm ; Broecker et al., 1979). Such a condition is unlikely to be reached in the future.

As mentioned earlier, the sediments lying below water depths of about 5000 m in the Atlantic Ocean and about 4500 m in the Pacific and Indian oceans are nearly devoid of $CaCO_3$ mainly because of pressure enhancement of $CaCO_3$ solubility. On the other hand, deep sea sediments located on the flanks of mid-ocean ridges and rises at water

depths shallower than about 4000 m contain as much as 80 wt% or more $CaCO_3$. The $CaCO_3$ content in the sediments in continental slope areas and inland sea basins varies over wide range, averaging about 25 wt%, because of dilution with detritus derived from the continents. The ocean floor areas shallower than 4000 m of water depths are lined with calcareous sediments several hundred meters or more thick. However, only a small fraction of these $CaCO_3$ should be available for the neutralization of the industrial CO_2 because of the buildup of clay-like residues at the ocean water-sediment boundary after the leaching of $CaCO_3$.

Assuming that the neutralization reaction takes place via molecular diffusion of carbonate ions through a layer of sediments saturated with water, and that the rate of the neutralization reaction is proportional to the CO_3^{2-} concentration in the pore water in the sediments, the characteristic depth in sediments, Z*, at which the concentration of CO_3^{2-} becomes halfway between that in the acidified ocean water and that at equilibrium with the $CaCO_3$ in the sediments may be expressed by

$$Z^* = (\ln 2)(t \cdot D/f)^{1/2}$$

where t is the resaturation time for a sediment composed entirely of $CaCO_3$, D is the molecular diffusivity of CO_3^{2-} in pore fluid (2×10^{-6} cm^2 s^{-1}), and f is the fraction of $CaCO_3$ in sediments (Takahashi and Broecker, 1977). The resaturation time, t, for the neutralization reaction has been estimated to be about 10 minutes for foraminifera shells in seawater. Thus, the characteristic depth for half neutralization should be about 1 millimeter. This suggests that if sediments remain undisturbed, the rate of neutralization reaction will be regulated mainly by the slow diffusion of CO_3^{-2} ions. Furthermore, as the accumulation of non-$CaCO_3$ residues has reached a centimeter or so of sediments, the neutralization reaction will be halted. However, the deep sea floor is constantly being stirred by burrowing organisms and other benthic dwellers in search of foods. The rate of this bioturbation process in sediments has been estimated using the vertical distribution of ^{210}Pb (decay half-life 22 years) and its parent nuclide ^{226}Ra (decay half-life 1620 years) in sediments (Nozaki et al., 1977; Peng et al., 1979b). The bioturbation process effectively mixes sediments down to about 10 cm deep. Peng and Broecker (1978) showed that the non-calcite residue will be stirred into the mixed layer with sufficient rapidity that its influence will not become significant until the mixed layer as a whole drops in calcite content. If the bioturbation is characterized as an eddy diffusive process, the diffusivity would be 5×10^{-7} cm^2 s^{-1}. This means that in 128 years, the sediments will be mixed down to an average depth of 4 cm, and in 512 years down to 8 cm. Therefore, the

bioturbation process should make the upper several centimeters of sediments available for the neutralization of industrial CO_2 during the next century.

The amount of $CaCO_3$ present in the upper 4.5 cm of oceanic sediments has been estimated to be about 20 x 10^{16} moles (Broecker and Takahashi, 1977a), 50% of which is located in the Atlantic Ocean basins. It has also been estimated that about 18 x 10^{16} moles of CO_2 will be released by industrial activities by the year 2100. Thus, these figures suggest that a sufficient amount of $CaCO_3$ will be available in the deep sea sediments for the neutralization of the industrial CO_2 which will be released into the ocean-atmosphere system during the next 120 or so years.

The beginning of $CaCO_3$ dissolution in deep sea sediments caused by anthropogenic CO_2, however, depends on both ocean ventilation rates and calcite dissolution rates. Based on ^{14}C dating of seawater, the ventilation times range up to 1500 years for the deep water in the North Pacific Ocean to about one hundred years for the deep water of western Atlantic Ocean basin (Broecker and Peng, 1982). This means it will take about a hundred to over a thousand years for a significant amount of surface acidified waters to reach the deep ocean. In addition, because of the slow diffusive processes for ions in deep sea sediments, the time constant for $CaCO_3$ dissolution has been estimated to be 1300 years (Broecker and Takahashi, 1977b). Hence, it will take on the order of thousands of years for $CaCO_3$ dissolution in deep sea sediments to become a significant factor in neutralizing anthropogenic CO_2.

Biological Carbon Pump

Biogenic materials produced in the euphotic zone of the oceans are largely recycled through the food chain in the upper oceans, and only about 10% of the total production falls to deep waters as fecal pellets and other forms of aggregates. This amount is called the "new production" (Dugdale and Goering, 1967). It represents the net down ward carbon flux exported to the deep ocean regime, where the organic matter is oxidized to CO_2, nitrate and phosphate.

The total primary photosynthetic production of the global oceans has been estimated to be between 20 and 45 x 10^{15} g C (1 x 10^{15} g C = 1 GtC) per year on the basis of the ^{14}C-labeled CO_2 incubation measurements (De Vooys, 1979). The new production of the world oceans may be roughly estimated to be about 3 x 10^{15} g C per year or about 10% of the total production on the basis of a simple steady-state box model calculation, in

which the amount of nutrient salts brought up to the euphotic zone by the upwelling of deep water at a mean rate of 4 m yr^{-1} is assumed to be balanced by the removal by the biological pump. Eppley and Peterson (1979) considered the rate of nitrate incorporation to be representative of the new production and estimated the ratio of the new production to the total production (the sum of the incorporation rates of nitrate, ammonium, urea, and other organic compounds) by using the ^{15}N-labeled nitrate. They estimated that the global new production is 18-20% of the total primary production, or 3.4-4.7 x 10^{15} g C per year. New production can also be estimated by the consumption rate of oxygen dissolved in seawater. Using the relationship observed between the concentration of dissolved oxygen in seawater and that of ^{3}He produced by radioactive decay of tritium, Jenkins (1982) and Jenkins and Goldman (1985) estimated the new production to be 4 mol·m^{-2}·yr^{-1} (or 48 g C $m^{-2}yr^{-1}$) in the temperate North Atlantic (i.e., Sargasso Sea). This value is nearly 30 times as large as that estimated by Eppley and Peterson (1979) in the oligotrophic waters of temperate gyre (1.5 g C $m^{-2}yr^{-1}$) and is about 7 times as large as that estimated in the transitional waters (7 g C $m^{-2}yr^{-1}$) between temperate gyre areas and subpolar zones. The new production rate in the temperate North Pacific Ocean has also been measured through the use of yet another method by Martin et al. (1987): free-floating particle traps, which are designed to collect gravitationally settling particles at several hundred meters in water depths. They obtained an estimate of 1.5 mol·m^{-2}·yr^{-1} (or 18 g C $m^{-2}yr^{-1}$) or about 14% of the total production. Although the new production is expected to vary widely with seasons and geographical locations, the values estimated through the various methods appear to disagree significantly. Obviously, further investigations are needed to reconcile the existing discrepancies.

Redfield (1934) examined the relationship between the concentrations of phosphate, nitrate, oxygen, and CO_2 dissolved in the surface and deep waters of the North Atlantic Ocean and observed that linear relationships exist between these concentrations. He attributed the observed relationships to the release into seawater of the oxidation products of biogenic debris with an elemental P:N:C ratio of 1:20:140 and to the consumption of 120 units of O_2. He supported this conclusion with the observation that this ratio is consistent with the P:N:C ratio of 1:18:137 for the mean elemental composition of marine plankton. This ratio was later revised (Redfield et al., 1963) to 1:16:106. Because oxygen may be utilized to oxidize carbon to yield CO_2 with a stoichiometric ratio of 1:1 and NH_4^- to yield NO_3^- with a ratio of 1:2, they assumed the O_2 utilization value of -138 units (= 106 + 2 x 16). This ratio has stood unchallenged for many years, and has been used extensively to characterize the biological pump in the oceans.

As more improved chemical data have become available in recent years, improved estimates for the stoichiometry of biogenic particulates have been obtained. On the basis of the changes in the concentrations of these salts and gases in seawater observed along selected constant density layers within the thermocline depths of the Atlantic and Indian oceans, a P:N:C:-O_2 ratio of 1:16:122 ($\pm$18):175 has been obtained (Takahashi et al., 1985). The uncertainty in the carbon ratio is due mainly to the lack of knowledge about the effect of the uptake of anthropogenic CO_2 in the ocean. Similar values have been observed in the deep waters of the Pacific and Indian oceans, the Norwegian and Greenland seas, and the Red Sea (Broecker et al., 1985b; Peng and Broecker, 1987).

Another independent estimate on these ratios may be provided from the samples of sinking biogenic debris collected from sediment traps. Based on the particle flux data obtained in the northeastern Pacific, Martin et al. (1987) observed that the biogenic debris is oxidized and releases the oxidized products to seawater with a stoichiometric ratio that increases with water depth. For example, the P:N:C:-O_2 ratio increased from 1:16:99:163 at 100 m deep, to 1:16:134:214 at 1000 m, and to 1:16:146:232 at 4000 m. The first two sets of values are consistent with the thermocline values estimated by Takahashi et al. (1985) in a depth range on the basis of the changes in chemical concentration in seawater. The observed change in the stoichiometric ratio as depth increases appears to suggest that the biogenic components that contain less carbon are oxidized first in shallower waters and those progressively richer in carbon are oxidized in deeper waters. Furthermore, although the elemental ratio observed in marine organic particulates settling through the water column varies from 4 to 20 for N:P and from 100 to 800 for C:P (Bishop et al., 1980; Honjo et al., 1982), the ratio observed in seawater is confined to a narrow range. This narrow range suggests that the chemical variability in the source materials tends to be smoothed out because the replacement time (about 1000 year) for these elements via the biological pump in the oceans is considerably longer than the time scale for lateral mixing of water.

The results of recent studies discussed above indicate that the amount of oxygen required to oxidize the marine biogenic debris is considerably greater than that proposed by Redfield et al. (1963) who assumed a 1:1 ratio of C:-O_2. These results also suggest that an extra amount of oxygen is needed to oxidize not only ammonia but also the excess hydrogen atoms in lipids, carbohydrates, and other organic compounds.

Geochemical Tracers in the Ocean

Reliable determination of the actual distribution of the CO_2 produced from burning fossil fuel up to any given time between the air and sea is a difficult task because of incomplete understanding of the three major controlling processes: CO_2 transfer across the sea-air interface, biological pump, and ocean water circulation and mixing. The spatial and temporal variabilities of the rates and distribution of these natural processes are not well understood. The geochemical tracers in the ocean can be used to study some of these processes.

Progress on understanding the rate at which ocean surface water is mixed into deeper layers of the ocean has been made recently through the use of radioactive and chemical tracers (see a review by Broecker, 1981). These tracers include (1) ^{90}Sr, ^{137}Cs, ^{85}Kr, and CFC's (chlorofluorocarbons); (2) ^{39}Ar, ^{222}Rn, ^{226}Ra, and ^{32}Si; and (3) ^{14}C, ^{3}H, and ^{3}He. Tracers in group (1) are entirely anthropogenic in origin and thus are transient tracers. Tracers in group (2) are entirely natural in origin and hence are steady-state tracers. Tracers in group (3) are partly anthropogenic and partly natural in origin. In the case of ^{3}H and ^{3}He, the anthropogenic component dominates in the upper oceans. For ^{14}C the man-made component constitutes about 20% of the total ^{14}C in surface waters and is negligible in deep water. The differences between tracers are sufficiently large that the information obtained from the distribution of one tracer is not redundant with that obtained from the distribution of another. Geochemical expeditions such as GEOSECS, TTO (Transient Tracers in the Ocean) and SAVE (South Atlantic Ventilation Experiments) programs have provided extensive information concerning the distribution of most of these tracers over the world oceans. Results show the penetration of bomb-produced tritium in the North Atlantic Ocean (Ostlund et al, 1976), the penetration of bomb-produced tritium into the thermocline region of the Atlantic and Indian Oceans (Broecker et al, 1980), characteristics of deep water formation in the North Atlantic via the distribution of CFCs in sea water (Bullister and Weiss, 1982), and the global distribution and vertical inventory of bomb-produced radiocarbon (Broecker et al. 1985a) and tritium (Broecker et al. 1986a). These tracer distributions have been used extensively for calibrating ocean mixing models which are used for estimating the uptake of anthropogenic CO_2.

Ocean Models

Because of the complexity and the dynamic nature of the oceanic CO_2 reservoir, mathematical models are essential tools for gaining an improved understanding of the oceanic CO_2

system and its interaction with the atmosphere. These models of the ocean-atmosphere system are also necessary for understanding the effects of the interactions of controlling processes for determining the CO_2 holding capacity of the ocean and the net flux of oceanic uptake of anthropogenic CO_2. The difficulties in modeling the ocean carbon cycle lies in realistically parameterizing these complexed natural processes including their rates and spatial-temporal variabilities.

Ocean models evolve and improve as new field data become available and understanding of the ocean-atmosphere dynamics increases. The most basic one-dimensional model of the ocean is the box-diffusion model proposed by Oeschger et al. (1975), a model which describes the world ocean in terms of a well-mixed surface layer (75 m) and a deep-sea reservoir, within which vertical transfer is described in terms of an eddy diffusivity. The rate of air-sea exchange is based on measurements of ^{14}C in the air and the sea, and the vertical mixing is characterized by a diffusivity constant of 1.25 $cm^2\ s^{-1}$, which yields a vertical distribution of natural ^{14}C consistent with the observed global average. Since the biological pump is implicitly assumed to be unchanged in this model, it is considered to be a perturbation model for the oceans.

There are a number of ocean models developed according to this basic box-diffusion structure with various modifications. For example, Peng et al. (1983) modified this model (Fig. 6) by adding explicit biological cycling and changing the eddy diffusivity to 1.6 $cm^2\ s^{-1}$ in the thermocline to account for the faster penetration of tritium during the period 1957-73. The biological pump is shown as wiggled arrows in Fig. 6. The nutrients (represented by PO_4 concentration) supplied to the surface water by the vertical mixing is assumed to be instantaneously and completely utilized by photosynthesis to form biogenic matter according to Redfield ratio (i.e., P:C = 1:122). This biogenic matter is assumed to pass through the food chain and eventually falls to lower layer as biogenic particulate, which is oxidized below the surface mixed layer and returns CO_2 and nutrient salts back to the water. The model yields a new production of 8.3 GtC yr^{-1}, which lies within the limits of values estimated on the basis of observations. The amount of organic matter oxidized decreases with depth following an assumed exponential function with half-oxidation depth of 400 m. In the polar regions, the surface water exposed to the atmosphere cools during the winter, increases density, and then sinks to the deep ocean. As shown by two advective arrows with polar outcrop box in Fig. 6, this process of deep water formation is simulated by downwelling of the cooled surface water and upwelling of subsurface water from the bottom ocean to the intermediate depth (i.e., 1000 m), from where the water rises to

the surface at polar regions. The upwelling water flux is assumed to be 50 x 10^6 m^3 s^{-1} (equivalent to a mean ocean upwelling rate of 4 m yr^{-1}), which has been estimated on the basis of the hydrological balance. This model reproduces satisfactorily the laterally averaged PO_4 and ^{14}C results of the GEOSECS survey.

Siegenthaler (1983) extended the box-diffusion model to include the role of intermediate and deep water formation at high latitudes. The deep sea is represented by a series of isopycnal layers that outcrop in the polar regions, which constitute about 10% of the global ocean surface. Lateral mixing is assumed to be instantaneous, and hence, the ventilation of deep sea becomes limited by the size of surface area of deep water formation at high latitudes and the rates of gas exchange.

Using the distribution of bomb-produced radiocarbon in the oceans as observed during the GEOSECS and TTO programs, Broecker et al. (1985a) proposed a lateral transport model of the global oceans. In this model, the world oceans are separated according to three major oceans - the Atlantic, the Pacific, and the Indian oceans. Within each ocean, it is divided into latitudinal zones based on the distribution of bomb-produced ^{14}C. As shown in Figure 7, the Atlantic and Pacific oceans are thus divided into 5 zones and the Indian ocean into 3 zones. The mixing within each latitudinal zone is described by a box-diffusion type of model. The vertical mixing rate for each zone is determined by the concentration of bomb-produced ^{14}C in the surface layer. The linkage between each zones is completed with schemes of upwelling and downwelling in water column coupled with a divergence or convergence in surface water flow. Based on the inventory of bomb-produced ^{14}C in each zone, the direction and the magnitude of the surface flow and of the vertical advective flow are determined. To satisfy the observed distribution of bomb-produced ^{14}C, upwelling process is required for tropical and Antarctic zones in oceans and for the northern zone of the Pacific Ocean. Correspondingly, it is necessary to call for a convergence of surface water flow coupled with downwelling in the temperate regions of all the oceans and in the northern Atlantic Ocean. This model assumes that deep water of each zone is not connected. The water upwelled from the bottom of the ocean is assumed to be free of bomb-produced ^{14}C. Using ^{3}H input function of Weiss and Roether (1980), this model also reproduces a reasonable global bomb-produced ^{3}H distribution in the ocean (Broecker et al. 1986a).

Two approaches are being pursued to develop more realistic three-dimensional ocean models. First, a general circulation model of the ocean has been developed on the basis of dynamical principles (Hasselmann, 1982) and used for the simulation of the transfer of

carbon and ^{14}C (Maier-Reimer and Hasselmann 1987, Bacastow and Maier-Reimer 1990). Radiocarbon distribution in the world's oceans has also been simulated (Toggweiler et al. 1989a and 1989b) by using the general circulation model based on primitive equations as developed by the Geophysical Fluid Dynamics Laboratory. These models have been used for estimating the uptake of CO_2 from fossil fuel (Sarmiento et al. 1992). Second, by an inverse method based on the observed quasi-steady distributions of temperature, salinity, total CO_2, alkalinity, ^{14}C, oxygen, and PO_4, Bolin et al. (1983) have obtained patterns of transfer parameters, using 12-box model of the oceans. However, verification against the transient changes that have occurred in recent years showed that the spatial resolution of their model was inadequate.

Estimates of CO_2 Uptake

One-dimensional ocean models have been used for computing the oceanic uptake of CO_2 (Peng, 1984 and 1986). To avoid uncertainties in the estimates of the ice-core-derived pCO_2 in the preindustrial atmosphere and to eliminate the uncertain contribution from the terrestrial biosphere, the observed atmospheric pCO_2 record at Mauna Loa Observatory (Bacastow and Keeling, 1981; Bolin, 1986) is used. In the calculation, the partial pressure of CO_2 in the atmosphere is prescribed in the model as input function. Values of model parameters and results of uptake calculation are summarized in Table 4. Computations are made with the box-diffusion model developed by Oeschger et al. (1975) with parameters derived from calibration with the distribution of natural ^{14}C and bomb-produced ^{14}C in the ocean. A modified box-diffusion model by Peng et al. (1983) and a lateral transport model by Broecker et al. (1985a) are also used.

When the fossil fuel CO_2 emission between 1958 and 1980 is taken to be 73.5×10^{14} mol, the original box-diffusion model of Oeschger et al. (1975) yields an oceanic uptake equivalent to 0.26 of total emission. When the same model calibrated with bomb-produced ^{14}C is used, it yields an oceanic uptake fraction of 0.34. The modified box-diffusion model of Peng et al. (1983) gives an oceanic uptake fraction of 0.29. Results from lateral transport models (Peng, 1986) indicate that the excess oceanic CO_2 is mainly distributed in the temperate regions of the world oceans and in the high latitude regions of the northern Atlantic where the North Atlantic Deep Water is formed. The global net uptake of excess CO_2 during this period is estimated to be about 35% of the fossil fuel CO_2 emission. In summary, if one-dimensional ocean models are used, the estimates of oceanic uptake range narrowly between 0.26 and 0.35 of the industrial CO_2 emission.

Recently, a three-dimensional global general circulation model of the world oceans has been adopted for studying the carbon cycle (Sarmiento et al. 1992). Using a perturbation approach, this model has been used for simulating the uptake of anthropogenic CO_2 by the ocean. The combined Siple ice core and Mauna Loa atmospheric pCO_2 records are prescribed in the model atmosphere for the period 1750-1990. Results of this simulation show that the average flux of CO_2 into the ocean is 1.9 GtC per year for the period 1980 to 1989. The estimated fossil fuel CO_2 emission during this period is 5.4 GtC each year. The oceanic uptake of fossil fuel CO_2 is thus estimated to be 35%, which is consistent with result obtained by lateral transport model.

The average airborne fraction between 1959 and 1978 was calculated to be 55% of fossil fuel CO_2 emission (Bacastow and Keeling, 1981). The remaining 45% of the CO_2 emission presumably was taken up by other carbon reservoirs. However, the 35% uptake calculated by the lateral transport models and lately by the more realistic ocean carbon perturbation model based on three-dimensional ocean GCM (Sarmiento et al. 1992) leaves 10% of the fossil fuel CO_2 emission unaccounted for. This imbalance may be caused either by the unrealistic design and calibration of the ocean models or by the failure to take into account other carbon sinks such as the terrestrial biosphere. Because these ocean models are based on the distribution of natural and bomb-produced ^{14}C in the global oceans, geochemists feel comfortable with the estimate of oceanic uptake and would look for extra sinks in the terrestrial biosphere. In contrast, however, terrestrial ecologists, based on land use data (Houghton et al. 1983), suggest that the land biota do not constitute a carbon sink but rather a significant and increasing source of atmospheric CO_2. Recently, based on the observed north-south CO_2 concentration gradient in the atmosphere and sea-air ΔpCO_2 data, Tans et al. (1990) proposed that a large amount of anthropogenic CO_2 is absorbed by the terrestrial ecosystems. These inconsistencies reflect the inadequate understanding of the global carbon cycle.

Terrestrial Biosphere

Based on the 1980-1989 IPCC (Intergovernmental Panel on Climate Change) budget for CO_2 perturbation (Houghton et al. 1990), the fossil fuel CO_2 emission is estimated to be 5.4 GtC $yr^{-1}$and deforestation release is 1.6 GtC yr^{-1}. The observed atmospheric CO_2 increase is averaged to be 3.4 GtC yr^{-1}. The average oceanic uptake is estimated to be 2.0 GtC yr^{-1}. Thus, the annual difference between carbon sources (a total of 7.0 $\pm$1.2 GtC) and sinks (a total of 5.4 $\pm$0.8 GtC) is 1.6 GtC, which represents the size of missing carbon sink yet to be accounted for.

The only other reservoir which is large enough and responsive enough to serve as a substantial sink for the missing carbon is the terrestrial biosphere which consists largely of wood in the forests and humus in the soils. For the wood-humus reservoir to house the missing carbon, some additional change must be causing trees to add thicker rings and soils to become richer in organic matter. For terrestrial biosphere to take up remaining 1.6 GtC each year, the increase in biomass or soil organic matter must more than compensate for the reduction caused by forestry and farming. If so, then the excess CO_2 in the atmosphere may be fertilizing plant growth (global greening) and causing a net increase in carbon stored in terrestrial system. Results of laboratory experiments carried out by plant physiologists show that on average the rate of growth of plants in the doubled CO_2 chamber is 1.35 times that of the control plants (Bazzaz and Fajer 1992). If these results were applied to plants in the real world, one would estimate that the 25% increase in atmospheric CO_2 which has occurred since the early 1800s should have caused plants to grow 9% faster. However, the limited supply of water and nutrients in real world situations will significantly reduce the impact on growth of the extra atmospheric CO_2. Besides, any additional growth must be stored in wood or soil humus and not released back to the atmosphere by normal death and decay. As in the case of the ocean, no means exists to directly measure the magnitude of the increases in carbon storage by the wood-humus reservoir. The only way is to compute it on basis of a balance between input and loss.

Using soil radiocarbon and carbon content profiles, Harrison and Broecker (1993) estimate that the global soil column contains about 450 GtC of fast-cycling carbon with a mean residence time of 25 years. Adjusting a greening factor of 1.35 according to time history of atmospheric CO_2 increase, they calculate the change in carbon storage in soil using a box model and obtain a net increase of 0.6 GtC per year for the 1980s. They also use a litter and fine root pool size of 110 GtC with a 3-year mean residence time. The annual increase is computed to be 0.3 GtC. With respect to vegetation biomass, they use a 1.5-year residence time for short-lived vegetation having a 90 GtC pool size and a 63-year residence time for a long-lived 500 GtC pool. Their estimates give 0.2 and 0.4 GtC sequestered annually for the short-lived and long-lived pools, respectively, as a result of CO_2 fertilization. Thus, a combined sink for terrestrial biosphere is estimated to be about 1.5 GtC per year. The result of this simple terrestrial model computation implies that terrestrial biosphere is a potential carbon sink that can account for most of the missing carbon.

Acknowledgment

Thanks to W. M. Post for reviewing and helping with technical arrangement of this manuscript. Work by T. Takahashi was performed for the Carbon Dioxide Research Program, Environmental Science Division, Office of Energy Research, U.S. Department of Energy, under subcontract No. 19X-SC428C with Lamont-Doherty Earth Observatory of Columbia University and with Martin Marietta Energy Systems, Inc., under contract DE-AC05-84OR21400. Research by T.-H. Peng at Oak Ridge National Laboratory was supported by the Carbon Dioxide Research Program, Environmental Science Division, Office of Energy Research, U.S. Department of Energy, under contract DE-AC05- 84OR21400 with Martin Marietta Energy Systems, Inc. Publication No.0000, Environmental Sciences Division, ORNL.

Table 1. CO_2 solubility and apparent dissociation constants of carbonic acid in sea water with a salinity of 35‰ under a total pressure of 1 atm and in pure water.

Temp. (°C)	CO_2 Solubility (10^{-2} mole/atm/kg)		First Diss. Const. (10^{-7})		Second Diss. Const. (10^{-11})	
	K_o	K_o'	K_1	K_1'	K_2	K_2'
2.0	7.714	5.822	2.801	6.634	2.52	3.59
25.0	3.406	2.839	4.452	9.965	4.68	7.77

Table 2 Mean temperature, salinity, alkalinity and total CO_2 concentration in the global oceans on the basis of the GEOSECS data (Takahashi et al., 1981a). The potential temperature (θ) indicates the temperature corrected for the adiabatic compression of a seawater at the pressure it is located.

Depth Range (meters)	Oceanographic Regimes	Potential Temp. (°C)	Salinity (‰)	Alkalinity (ueq/kg)	Total CO_2 (umol/kg)
0 - 50*	Surface mixed layer	19.2	34.9	2322	2012
50 - 1200*	Main thermocline	9.1	34.8	2332	2181
> 1200*	Deep Ocean	1.5	34.76	2390	2284
0 - 6000*	Whole Ocean**	3.9	34.78	2372	2251

* Area-weighted arithmetic mean. The following weighting factors have been used for each of the seven oceanic regions.

North Atlantic = 11.9% North Pacific = 21.9% North Indian = 3.4%
South Atlantic = 9.7% South Pacific = 21.4% South Indian = 13.6%
Antarctic (South of 45°S) = 18.2%

** Volume-weighted arithmetic mean. The mean world ocean depth of 4100 meters, and the following areal percentage for each depth range have been used.
0 - 50 = 100% of the oceanic area
50 - 1200 = 99.3% of the oceanic area
>1200 = 93.9% of the oceanic area

Table 3. Estimates of sea-air CO_2 flux (GtC per year) based on seasonal and annual mean ΔpCO_2 (μatm) reported by Tans et al. (1990).

Ocean	Location	January to April		July to October		Annual Mean	
		ΔpCO_2	Flux	ΔpCO_2	Flux	ΔpCO_2	Flux
Atlantic subartic	>50°N; 90°W to 20°E	-22	-0.15	-53	-0.31	-37	-0.23
Atlantic gyre	15°N to 50°N; 90°W to 20°E	-29	-0.58	-1	-0.02	-15	-0.30
North Pacific	>15°N; 110°E to 90°W	-11	-0.44	14	0.33	2	-0.06
Equatorial	15°S to 15°N; 180°W to 180°E	37	1.56	28	1.69	33	1.62
Southern gyres	50°S to 15°S; 180°W to 180°E	-9	-1.46	-25	-3.31	-17	-2.39
Antarctic	>50°S	-23	-0.38	-10	-0.03	-17	-0.20
Global		3	-1.5	-1	-1.7	1	-1.6

TABLE 4

Comparison of net fossil fuel CO_2 uptakes between 1958 and 1980 by various geochemical models of the ocean using Mauna Loa pCO_2 record as an input function*

Models	K (cm^2/s)	I (mol/m^2yr)	Net Uptake (10^{14} mol)	Fraction uptake
Box-diffusion (1)	1.25	18.0	19.4	0.26
Box-diffusion (2)	2.44	20.6	25.3	0.34
Modified box-diffusion (Peng et al 1983)	1.6	17.5	21.2	0.29
Lateral transport	---	---	26.0	0.35

* K = vertical diffusivity, I = CO_2 exchange rate. Box diffusion (1) is calibrated with natural ^{14}C and box diffusion (2) is calibrated with bomb-produced ^{14}C. The fraction of ocean uptake is calculated using the net production of fossil fuel carbon between 1958 and 1980 of 73.5 x 10^{14} moles.

FIGURE CAPTIONS

Fig. 1 - The depth distribution of the total CO_2 (TCO_2) concentration and total alkalinity (TALK) in the global oceans (Takahashi et al., 1981a). The global oceans are divided into seven regions: NA = North Atlantic; SA = South Atlantic; NP = North Pacific; SP = South Pacific; NI = North Indian; SI = South Indian; and AA = Antarctic region (South of 45°S).

Fig. 2 - The depth distribution of the CO_3^{-2} ion in various oceanic regions and the solubility curves for calcite (CC) and aragonite (CA) in seawater. The letters along the regional mean curves indicate the following: NA = North Atlantic; SA = South Atlantic; NP = North Pacific; SP = South Pacific; NI = North Indian; SI = South Indian; AA = Antarctic region (South of 45°S); and WM = World mean.

Fig. 3 - The effect of wind speed (at 10 m above the sea surface) on the sea-air gas transfer piston velocity (Vp) for various gases. The Vp values are corrected to a Schmidt number of 600, which corresponds to CO_2 gas at 20°C. The circles indicate the mean values obtained using the radon deficiency measurements in oceans, and the squares indicate the values estimated on the basis of ^{14}C concentrations in the air and seawater. The long-dashed line indicates the upper limit of the wind tunnel data; the short-dashed line indicates the relationship used in this study. The solid lines indicate the lower limit of the wind tunnel data, which are consistent with the values obtained by using SF_6 as a gas exchange tracer in a lake environment (Wanninkhof et al., 1985). This figure was modified from Liss and Merlivat (1986).

Fig. 4 - The distribution of the sea-air pCO_2 difference over the global oceans measured during the 1972-78 GEOSECS program. The sea-air pCO_2 difference is expressed in micro-atmospheres. The positive values indicate that the net transfer of CO_2 is from the sea to the air, and hence the sea is a source for atmospheric CO_2. The negative values indicate that the net transfer is from the air to the sea, and hence the sea is a CO_2 sink.

Fig. 5 - The mean pCO_2 values in the surface water of the Sargasso Sea, North Atlantic Ocean, observed during the three major expeditions in 1957, 1972-73 and 1982. The values are normalized to the mean temperature 19.6°C of the Sargasso Sea surface water observed in 1982. The atmospheric pCO_2 values have been computed from the atmospheric CO_2 concentration (mole fraction of CO_2 in dry air, fCO_2) observed

at Mauna Loa Observatory, Hawaii, by Bacastow and Keeling (1981); the equilibrium water vapor pressure (PH_2O) of 0.022 atm at 19.6°C; and the total barometric pressure (Pb) of 1.000 atm in the following equation:

$$pCO_2\ (\mu atm)\ \text{in air} = fCO_2\ (Pb(atm) - PH_2O(atm)).$$

The seawater pCO_2 values are about 15 μatm lower than the atmospheric pCO_2 values and have increased at a similar rate as the atmospheric pCO_2 value.

Fig. 6 - Modified box-diffusion model of the ocean (Peng et al. 1983). In addition to including eddy diffusive mixing through the water column, it also includes upwelling (water at polar outcrop sinks to the bottom ocean and upwells from there to the mid-depth) and biological pumping (wiggled arrows which show the organic particulates are formed in the surface layer and oxidized in the lower layers as they fall). The box numbers are shown in the center of the diagram. The thickness of each box is 50 m, with surface mixed layer of 100 m and the total water column of 3800 m.

Fig. 7 - Diagram of the simplified lateral transport model for simulation of the distribution of bomb-produced ^{14}C in the ocean. Three major oceans are divided into latitudinal zones independently according to the observed distribution of bomb-produced ^{14}C in each ocean. The water fluxes shown in the diagram are vertical and horizontal advective flow and are given in Sverdrups ($1 \times 10^6\ m^3\ s^{-1}$). The lateral transport is assumed to take place only in the surface layers. These latitudinal zones are not connected in the deep layers. Waters upwell from the bottom of the ocean are assumed to be free of bomb-produced ^{14}C. Although the vertical mixing processes are not shown, they vary in each latitudinal zones in each ocean and an appropriate mixing rate is included in every water column for the computation of ^{14}C distribution and CO_2 uptake (see Peng 1986).

Fig. 1

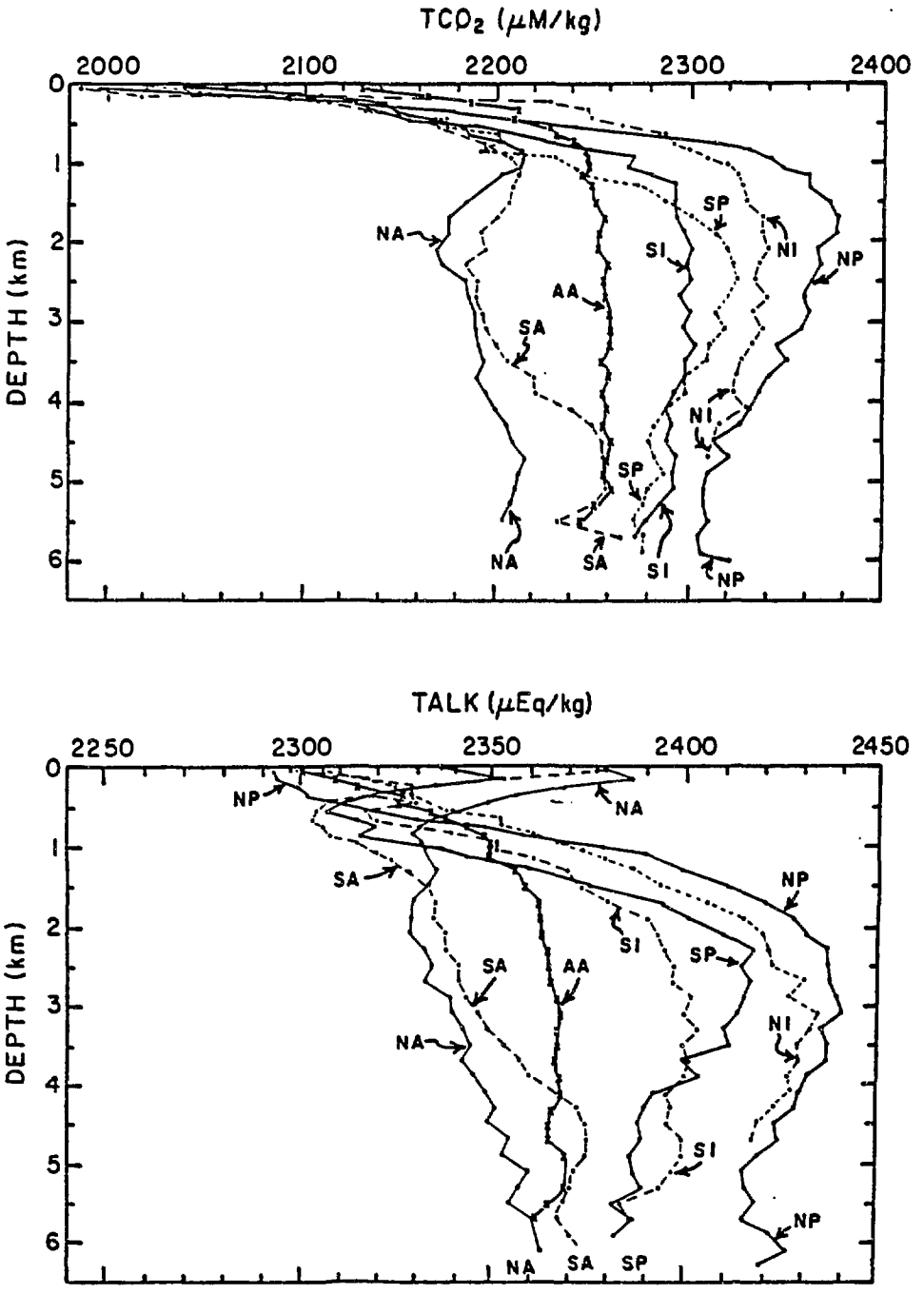
TCO2 (μM/kg)
2000
2100
2200
2300
2400
DEPTH (km)
0
1
2
3
4
5
6
NA
SP
SI
NI
NP
AA
SA
TALK (μEq/kg)
2250
2300
2350
2400
2450

Fig. 2

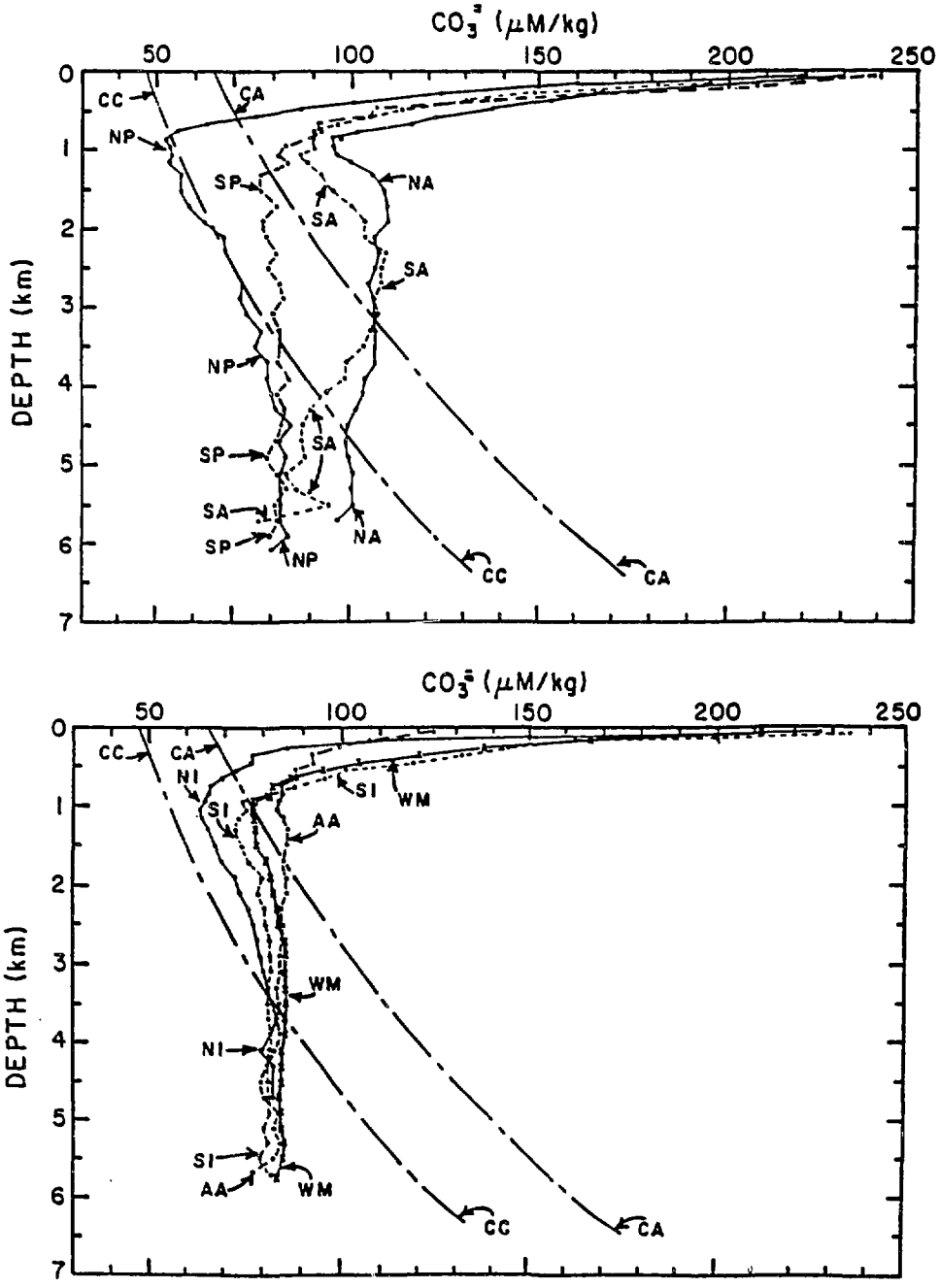
$CO_3^{=}$ (μM/kg)
50
100
150
200
250
DEPTH (km)
0
1
2
3
4
5
6
7
CC
CA
NP
SP
SA
NA
$CO_3^{=}$ (μM/kg)
CC
CA
NI
SI
WM
AA
NI
SI
AA
WM
CC
CA

Fig. 3

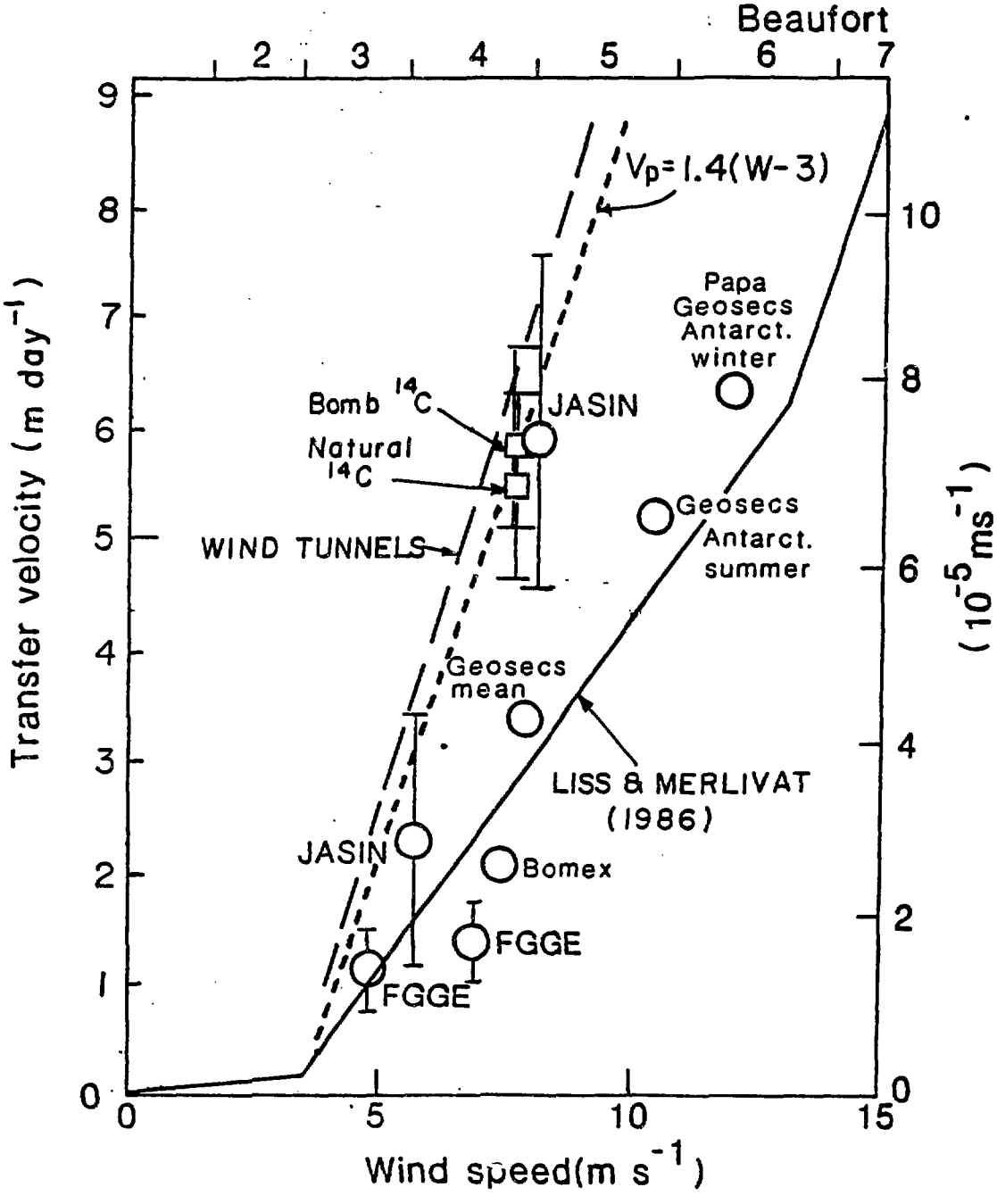
Beaufort
2
3
4
5
6
7
$V_p = 1.4(W-3)$
Papa
Geosecs
Antarct.
winter
Bomb ^{14}C
JASIN
Natural
^{14}C
Geosecs
Antarct.
summer
WIND TUNNELS
Geosecs
mean
LISS & MERLIVAT
(1986)
JASIN
Bomex
FGGE
FGGE
Transfer velocity (m day^{-1})
$(10^{-5}$ ms$^{-1})$
Wind speed(m s^{-1})
0
5
10
15

Fig. 4

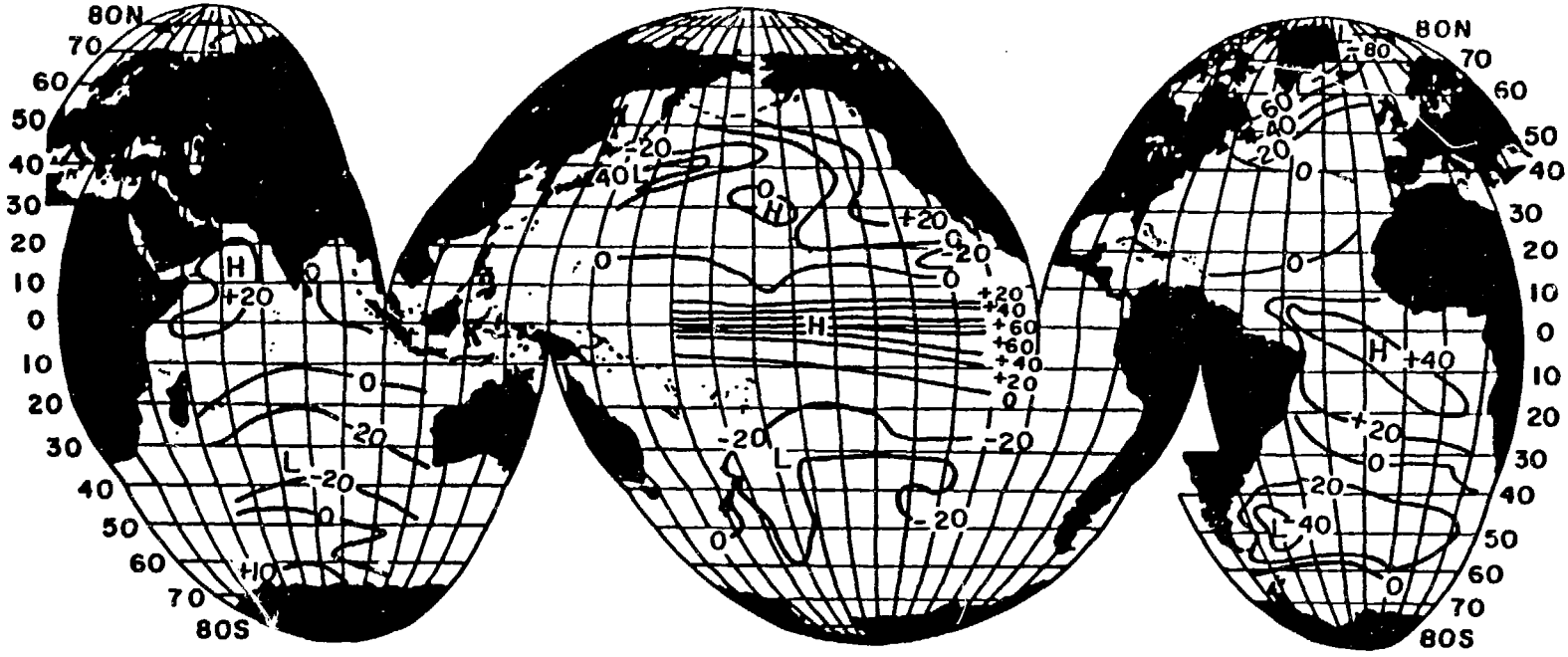
80N
70
60
50
40
30
20
10
0
10
20
30
40
50
60
70
80S
H
+20
0
-20
L
-40
+40
+60
+80

Fig. 5

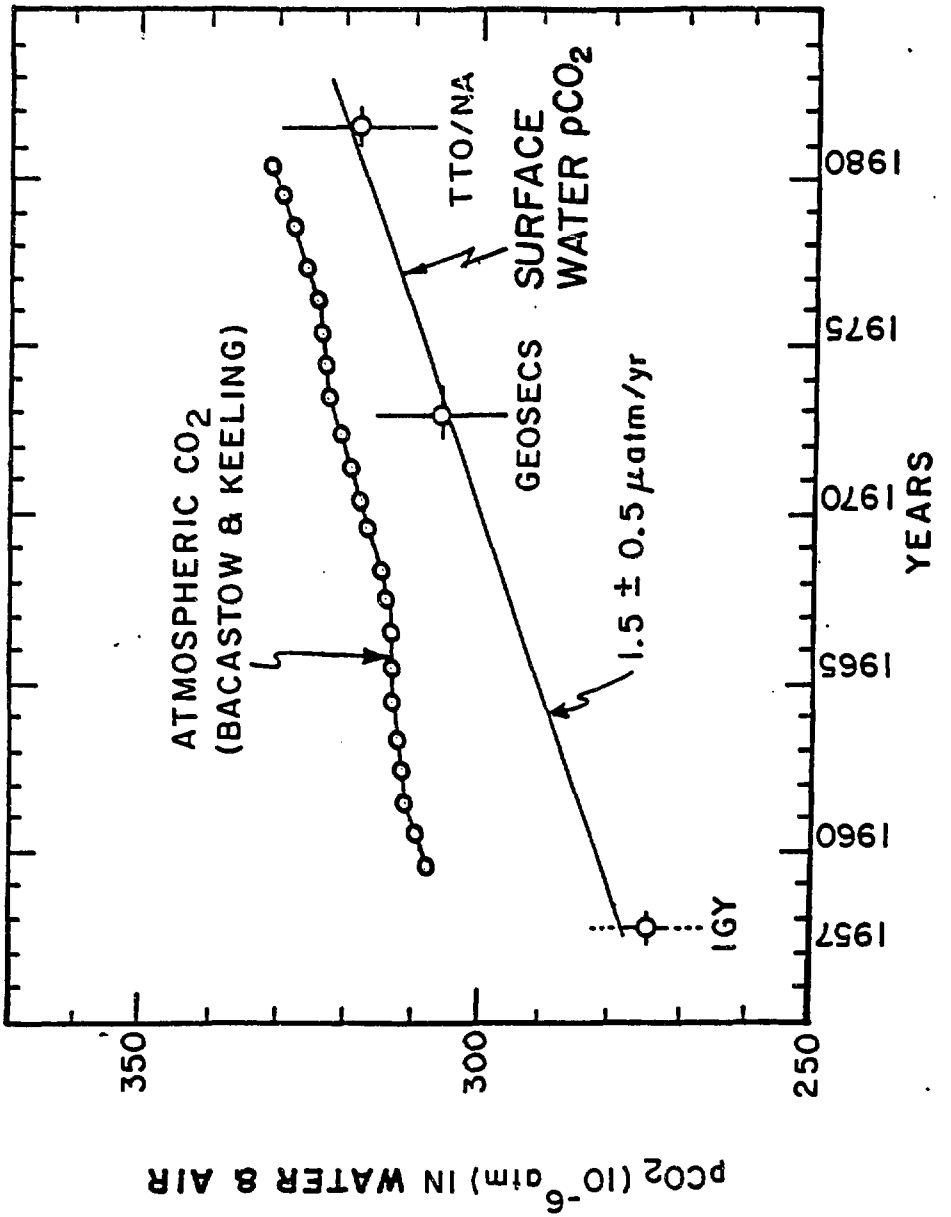
pCO2 (10-6atm) IN WATER & AIR
350
300
250
1957
1960
1965
1970
1975
1980
YEARS
IGY
1.5 ± 0.5 µatm/yr
GEOSECS
TTO/NA
SURFACE WATER pCO2
ATMOSPHERIC CO2 (BACASTOW & KEELING)

ORNL-DWG 89M-1874

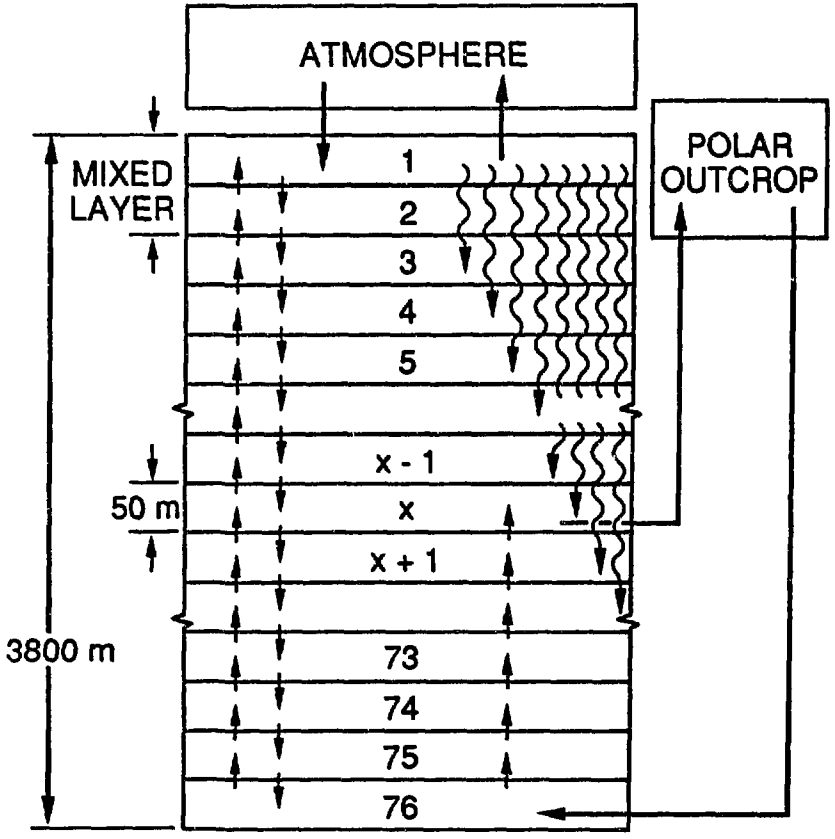

ATLANTIC

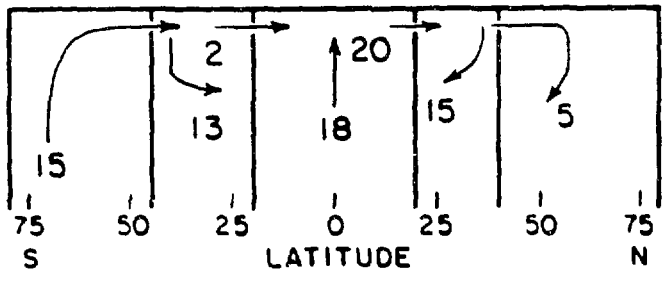

INDIAN

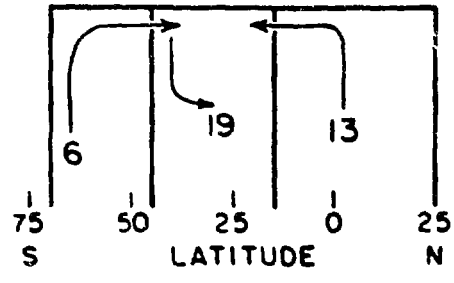

PACIFIC

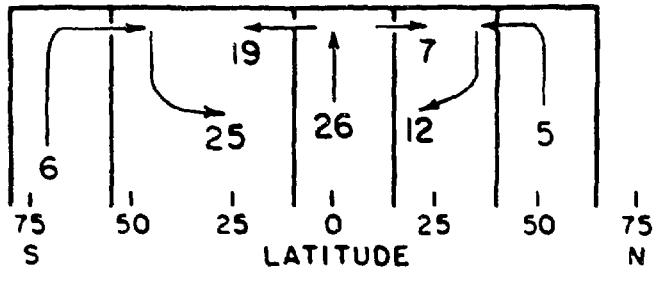

REFERENCES

Bacastow, R. B. and Keeling, C. D. (1981). Atmospheric carbon dioxide concentration and the observed airborne fraction. In "Carbon Cycle Modelling", B. Bolin editor, SCOPE 16, John Wiley & Sons, New York, 103-116.

Bacastow, R. B. and Maier-Reimer, E. (1990). Ocean-circulation model of the carbon cycle, Clim. Dyn., 4, 95-125.

Bates, R. G. and Culberson, C. H. (1977). Hydrogen ions and the thermodynamic state of marine systems. In "The Fate of Fossil Fuel CO_2 in the Oceans", N. R. Andersen and A. Malahoff editors, Plenum Press, N.Y., 45-61.

Bazzaz, F.A. and Fajer, E.D. (1992). Plant life in a CO_2 rich world, Sci. Am., 266, 68-74.

Bishop, J. K. B., Collier, R. W., Kettens, D. R. and Edmond, J. M. (1980). The chemistry, biology and vertical flux of particulate matter from the upper 1500 m of the Panama Basin. Deep-Sea Res., 27A, 615-640.

Bolin, B., Bjorkstrom, A., Holmen, K., and Moore, B. (1983). The simultaneous use of tracers for ocean circulation studies, Tellus 35B, 206- 236.

Bolin, B., (1986). How much CO_2 will remain in the atmosphere, in Bolin, B., Doos, B. R., Jager, J. (eds.), The Greenhouse Effect, Climatic Change, and Ecosystems, SCOPE 29, John Wiley & Sons, Chichester, 93-155.

Bradshaw, A. L., Brewer, P. G., Schaefer, D. K. and Williams, R. T. (1981). Measurement of total carbon dioxide and alkalinity by potentiometric titration in the GEOSECS Program, Earth and Planet. Sci. Letters, 55, 99-115.

Brewer, P. G. and Goldman, J. C. (1976). Alkalinity changes generated by phytoplankton growth. Lim. and Oceanogr., 21, 108-117.

Broecker, W. S. (1963). Radioisotopes and large-scale oceanic mixing. In "The Sea", Vol. 2, M. N. Hill editor, Interscience Pub., N.Y., 88-108.

Broecker, W. S. and Takahashi, T. (1966). Calcium carbonate precipitation on the Bahama Banks. Jour. Geophys. Res., 71, 1575-1602.

Broecker, W. S. and Y. -H. Li, (1970). Interchange of water between the major oceans. J. Geophys. Res. V75, p.3545-3552.

Broecker, W. S. and Takahashi, T. (1977a). Neutralization of fossil fuel CO_2 by marine calcium carbonate. In: The Fate of Fossil Fuel CO_2 in the Oceans, ed. by N. r. Andersen and A. Malahoff, Plenum Press, New York, 213-241.

Broecker, W. S. and Takahashi, T. (1977b). The solubility of calcite in seawater. In "Thermodynamics in Geology", D.G. Fraser, editor, D. Reidel Pub. Co., Dordrecht, Holland, 369-379.

Broecker W. S. and Takahashi, T. (1978). The relationship between lysocline depths and in situ carbonate ion concentration. Deep-Sea Res., 25, 65-95.

Broecker, W. S. (1979). A revised age for the radiocarbon age of North Atlantic Deep-Water. Jour. Geophys. Res., 84, 3218-3226.

Broecker, W. S., Takahashi, T., Simpson, H. J. and Peng, T.-H. (1979). Fate of fossil fuel carbon dioxide and the global carbon budget. Science, 206, 408-418.

Broecker, W. S., T.-H. Peng and R. Engh, (1980). Modeling the carbon system, Radiocarbon 22, 565-598.

Broecker, W. S. (1981). Geochemical tracers and ocean circulation, in B. A. Warren and C. Wunsch (eds.) Evolution of Physical Oceanography, The MIT Press, Cambridge, 434-461.

Broecker, W. S. and T. -H. Peng, (1982). TRACERS IN THE SEA, Eldigio Press, Palisades, New York, 690p.

Broecker, W. S., T. -H. Peng, G. Ostlund, and M. Stuiver, (1985a). The distribution of bomb radiocarbon in the ocean, J. Geophys. Res. V90, p.6953-6970.

Broecker, W. S., Takahashi, T. and Takahashi, T. (1985b). Sources and flow patterns of deep-ocean waters as deduced from potential temperature, salinity and initial phosphate concentrations, Jour. Geophys. Res., 90, 6925-6939.

Broecker, W. S., T. -H. Peng, and G. Ostlund, (1986a). The distribution of bomb tritium in the ocean, J. Geophys. Res. V91, p.14331-14344.

Broecker, W. S., Ledwell, J. R., Takahashi, T., Weiss, R. F., Merlivat, L., Memery, L., Peng, T.-H., Jahne, B. and Munnich, K. O. (1986b). Isotopic versus micrometeorologic ocean CO_2 fluxes: a serious conflict. Jour. Geophys. Res., 91, 10,517-10,527.

Bullister, J. L. and R. F. Weiss, (1982). Anthropogenic chlorofluoro- methanes in the Greenland and Norwegian Seas, Science 221, 265-268.

De Vooys, C. G. N. (1979). Primary production in aquatic environments, In "The Global Carbon Cycles", B. Bolin editor, SCOPE Vol. 13, J. Wiley & Sons, N.Y., 259-292.

Dugdale, R. C. and Goering, J. J. (1967). Uptake of new and regenerated forms of nitrogen in primary productivity. Limnol. and Oceanogr., 12, 196-206.

Eppley, R. W. and Peterson, B. J. (1979). Particulate organic matter flux and planktonic new production in the deep ocean. Nature, 282, 677-680.

Esbensen, S. K. and Koshnir, Y. (1981). The heat budget of the global ocean: An atlas based on estimates from the surface marine observations. Climatic Research Institute Report #29, Oregon State University, Corvalis, OR.

Garrels, R. M. and Christ, C. L. (1965). Solutions, Minerals and Equilibria. Harper & Row, New York, pp. 450.

Garrels, R. M. and Thompson, M. E. (1962). A chemical model for seawater at 25°C and one atmosphere total pressure. Am. Jour. Sci., 260, 57-66.

Gran, G. (1952). Determination of the equivalence point in potentiometric titrations, 2. Analysist, 77, 661-671.

Harned, H. S. and Davis, R. (1943). The ionization constant of carbonic acid in water and the solubility of carbon dioxide in water and aqueous salt solutions from 0° to 50°C. Jour. Am. Chem. Soc., 65, 2030-2037.

Harned, H. S. and Scholes, S. R. (1941). The ionization constant of HCO_3^{-1} from 0° to 50°C. Jour. Am. Chem. Soc., 63, 1706-1709.

Harrison, K., Broecker, W. S., and Bonani, G. (1993). A strategy for estimating the impact of CO_2 fertilization on soil carbon storage, Global Biogeochem. Cycles, 7, 69-80.

Hasselmann, K. (1982). An ocean model for climate variability studies. Progress in Oceanography 11, 69-92.

Honjo, S., Manganini, S. J. and Cole, J. J. (1982). Sedimentation of biogenic matter in the deep ocean. Deep-Sea Res., 29, 609-625.

Houghton, R. A., Hobbie, J. E., Melillo, J. M., Moore, B., Peterson, B. J., Shaver, G. R., and Woodwell, G., M. (1983). Changes in the carbon content of terrestrial biota and soils between 1860 and 1980: net release of CO_2 to the atmosphere. Ecological Monographs 53, 235-262.

Houghton, J. T. , Jenkins, G.J., and Ephraums, J.J. (1990). Climate Change, The IPCC Scientific Assessment, Cambridge Press, New York, 365pp.

Ingle, S. E., Culberson, C. H., Hawley, J. E. and Pytkowicz, R. M. (1973). The solubility of calcite in seawater at atmospheric pressure and 35 $^{\circ}/_{oo}$ salinity. Marine Chem., 1, 295-307.

Ingle, S. E. (1975). Solubility of calcite in the ocean. Marine Chem., 3, 301-319.

Jenkins, W.J. (1982). Oxygen utilization rates in North Atlantic subtropical gyre and primary production in oligotrophic systems. Nature, 300, 246-248.

Jenkins, W. J. and Goldman, J. C. (1985). Seasonal oxygen cycling and primary production in the Sargasso Sea, Jour. Marine Res., 43, 465-491.

Klein, J., J. C. Lerman, P. E. Damon, and E. K. Ralph, (1982). Calibration of radiocarbon dates: Tables based on the consensus data of the Workshop on Calibrating the Radiocarbon Time Scale, Radiocarbon 24, 103-150.

Liss, P. S. and Merlivat, L. (1986). Air-sea gas exchange rates: introduction and synthesis. In "The Role of Air-Sea Exchange in Geochemical Cycling", P. Buat-Menard editor, D. Reidel Publishing Co., Dordrecht, Holland, 113-127.

Maier-Reimer, E. and K. Hasselmann. (1987). Transport and storage of CO_2 in the ocean - an inorganic ocean-circulation carbon cycle model, Climate Dynamics 2, 63-90.

Martin, J. H., Knauer, G. A., Karl, D. M. and Broenkow, W. W. (1987). VERTEX: carbon cycling in the northeast Pacific. Deep-Sea Res., 34, 267-285.

Millero, F. J. (1979). The thermodynamics of the carbonate system in seawater. Geochim. et Cosmochim. Acta, 43, 1651-1661.

Murray, C. N. and Riley, J. P. (1971). The solubility of gases in distilled water and sea water - IV. Carbon dioxide. Deep-Sea Res., 18, 533-541.

Nozaki, Y., Cochran, J. K., Turekian, K. K., and Keller, G. 1977. Radiocarbon and ^{210}Pb distribution in submersible-taken deep-sea cores from Project FAMOUS, Earth Planet. Sci. lett., 34, 167-173.

Nydal, R. and Lovseth, K. (1983). Tracing bomb ^{14}C in the atmosphere (1962-1980), J. Geophys. Res. 88, 3621-3642.

Oeschger, H.. Siegenthaler, U., and Gugelmann, A. (1975). A box diffusion model to study the carbon dioxide exchange in nature. Tellus 27, 168-192.

Ostlund, H. G., H. G. Doresy, and R. Brescher, (1976). GEOSECS Atlantic Radiocarbon and Tritium Results, Tritium Lab. Data Report No. 8, Rosenstiel School of Marine and Atmospheric Science, University of Miami, Miami, Florida, pp.14.

Ostlund, H. G. and Stuiver, M. (1980). GOESECS Pacific radiocarbon. Radiocarbon, 22, 25-53.

Ostlund, H. G. 1985. Tritium and radiocarbon in the North Atlantic Ocean, An Overview. J. Of the Marine Res. Institute Reykjavik, 9, 13-19.

Peng, T.-H., and W. S. Broecker. 1978. Effect of sediment mixing on calcite dissolution by fossil fuel CO_2, Geophys. Res. Lett. 5, 349-352.

Peng, T.-H., W. S. Broecker, G. G. Mathieu, and Y.-H. Li. (1979a). Radon evasion rates in the Atlantic and Pacific Oceans as determined during GEOSECS program. J. Geophysical Research. 84:2471-2486.

Peng, T.-H., W. S. Broecker, and W. H. Berger. (1979b). Rates of benthic mixing in deep sea sediment as determined by radiocarbon tracers. Quaternary Res. 11, 141-149.

Peng, T.-H., W. S. Broecker, H. D. Freyer, and S. Trumbore. (1983). A deconvolution of the tree rings based $\delta^{13}C$ record. J. Geophysical Research 88:3609-3620.

Peng, T.-H. (1984). Invasion of fossil fuel CO_2 into the ocean. In: Gas Transfer at Water Surfaces, edited by W. Brutsaert and G. D. Jirka, D. Reidel Publ. Company, Dordrecht, Holland, pp. 515-523.

Peng, T.-H. (1986). Uptake of Anthropogenic CO_2 by Lateral Transport Models of the Ocean Based on the Distribution of Bomb-Produced ^{14}C. Radiocarbon 28, p.363-375.

Peng, T.-H. , Takahashi, T., Broecker, W. S. and Olafsson, J. (1987). Seasonal variability of carbon dioxide, nutrients and oxygen in the northern North Atlantic surface water: Tellus, 39B, 439-458.

Peng, T. -H. and W. S. Broecker. 1987. C/P ratios in Marine Detritus, Global Biogeochem. Cycles, Vol. 1, p.155-161.

Redfield, A. C. (1934). On the proportions of organic derivatives in sea water and their relation to the composition of plankton. in "James Johns Memorial Volume", Liverpool, U.K.,177-192.

Redfield, A. C., Ketchum , B. H. and Richards, F. A. (1963). The influence of organisms on the composition of sea water. In "The Sea", Vol. 2, M. N. Hill editor, Interscience Publ., N.Y., 26-77.

Revelle, R. and Suess, H. (1957). Carbon dioxide exchange between atmosphere and ocean, and the question of an increased atmospheric CO_2 during the past decades. Tellus, 9, 18-27.

Roether, W. and Kromer, B. (1984). Optimum application of the radon deficit method to obtain air-sea gas exchange rates. In "Gas Transfer at Water Surfaces", W. Brutsaert and G. H. Jirka editors, D. Reidel Publishing Co., Holland, 447-457.

Siegenthaler, U. (1983). Uptake of excess CO_2 by an outcrop-diffusion model of the ocean. Journal of Geophysical Research 88C6, 3599-3608.

Simpson, H. J. and Takahashi, T. (1973). Chemical model of seawater and saline waters. Initial report of the Deep Sea Drilling Project, Vol. XX, U.S. Government Printing Office, Washington, D.C., 877-886.

Stuiver, M. (1980). ^{14}C distribution in the Atlantic Ocean, J. Geophys. Res., 85, 2711-2718.

Takahashi, T. (1975). Carbonate chemistry of seawater and the calcite compensation depth in the oceans. Special Pub. 13, Cushman Foundation for Foraminiferal Res., Washington, D.C., 11-26.

Takahashi, T. and Broecker, W. S. (1977). Mechanisms for calcite dissolution on the sea floor. In: The Fate of Fossil Fuel CO_2 in the Oceans, ed. by N. r. Andersen and A. Malahoff, Plenum Press, New York, 455- 477.

Takahashi, T. , Broecker, W. S., Werner, S. R. and Bainbridge, A. E. (1980). Carbonate chemistry of the surface waters of the world oceans. In "Isotope Marine Chemistry", E.D. Goldberg, Y. Horibe and K. Saruhashi editors, Uchida-rokaku-ho, Tokyo, Japan, 291-326.

Takahashi, T., Broecker, W. S. and Bainbridge, A. E. (1981a). The alkalinity and total carbon dioxide concentration in the world oceans. In "Carbon Cycle Modelling", B. Bolin editor, SCOPE 16, John Wiley & Sons, New York, 271-286.

Takahashi, T., Broecker, W. S. and Bainbridge, A. E. (1981b). Supplement to the alkalinity and total carbon dioxide concentration in the world oceans. In "Carbon Cycle Modelling", B. Bolin editor, SCOPE 16, John Wiley & Sons, New York, 159-199.

Takahashi,T., Chipman, D., Schechtman, N., Goddard, J., Wanninkof, R. (1982). Measurements of the partial pressure of C02 in discrete water samples during the North Atlantic Expedition, The Transient Tracers of Oceans Project. Technical Report to the National Science Foundation, Lamont-Doherty Geological Observatory, Palisades, N.Y., pp.268.

Takahashi, T., Chipman, D. and Volk, T.(1983). Geographical, seasonal and secular variations of the partial pressure of CO_2 in surface waters of the North Atlantic Ocean: the results of the North Atlantic TTO Program. In "Proceedings: Carbon Dioxide Research Conference: Carbon Dioxide, Science and Consensus", CONF-820970, U.S. Department of Energy, Washington, D.C., II.123-II.145.

Takahashi, T., Broecker, W. S. and Langer, S. (1985). Redfield ratio based on chemical data from isopycnal surfaces. Jour. Geophys. Res., 90, 6907-6924

Toggweiler, J. R., K. Dixon, and K. Bryan, (1989a). Simulations of radiocarbon in a coarse-resolution, world ocean model I: Steady state, pre-bomb distributions, J. Geophys. Res. 94, 8217-8242.

Toggweiler, J. R., K. Dixon, and K. Bryan, (1989b). Simulations of radiocarbon in a coarse-resolution, world ocean model II: Distribution of bomb-produced ^{14}C, J. Geophys. Res. 94, 8243-8264.

Weiss, R. F. (1974). Carbon dioxide in water and seawater: The solubility of a non-ideal gas, Marine Chem., 2, 203-215.

Weiss, R. F. (1981). Determinations of CO_2 and methane by dual catalyst flame ionization chromatography and nitrous oxide by electron capture chromatography. Jour. of Chromato r. Sci., 19. 611-616.

Weiss, W. and Roether, W. (1980). The rates of tritium input to the world oceans, Earth Planet. Sci. Lett., 49, 435-446.

Wanninkhof, R., Ledwell, J. R., and Broecker, W. S. (1985). Gas exchange - wind speed relation measured with sulfur hexafluoride on a lake. Science, 227, 1224-1226.